

From the Top: Surface-derived Carbon Fuels Greenhouse Gas Production at Depth in a Neotropical Peatland

Alexandra Hedgpeth^{1,2}, Alison M. Hoyt³, Kyle Cavanaugh¹, Karis J. McFarlane^{2*}, Daniela F. Cusack^{1,4,5*}

5 ¹Geography Department, University of California Los Angeles, Los Angeles, 94143, USA

²Lawrence Livermore National Laboratory, Livermore, 94550, USA

³Department of Earth System Science, Stanford University, Stanford, 94305, USA

⁴Department of Ecosystem Science & Sustainability, Colorado State University, Fort Collins, 80523, USA

⁵Smithsonian Tropical Research Institute, Balboa, Ancon, Republic of Panama, 0843-03092

10

★ These authors contributed equally to this work

Correspondence: Alexandra Hedgpeth (hedgpea10@g.ucla.edu)

Abstract.

15 Tropical peatlands play an important role in global carbon (C) cycling but little is known about factors driving carbon dioxide (CO₂) and methane (CH₄) emissions from these ecosystems, especially production in deeper soils. This study aimed to identify source material and processes regulating C emissions originating deep in three sites in a Neotropical peatland on the Caribbean coast of Panama. We hypothesized that: 1) surface derived organic matter transported down the soil profile is the primary C source for respiration products at depth; and 2) high lignin content results in hydrogenotrophic methanogenesis as the dominant
20 CH₄ production pathway throughout the profile. We used radiocarbon isotopic values to determine whether CO₂ and CH₄ at depth are produced from modern substrates or ancient deep peat, and we used stable C isotopes to identify the dominant CH₄ production pathway. Peat organic chemistry was characterized using ¹³C solid state nuclear magnetic resonance spectroscopy (¹³C-NMR). We found that deep peat respiration products had radiocarbon signatures that were more similar to surface dissolved organic C (DOC) than deep solid peat, even though the peat chemistry remained relatively stable from the surface
25 to the deeper layers. These results indicate that surface derived organic matter was the dominant source for gas production at depth in this peatland, likely because of vertical transport of DOC from the surface to depth. Lignin, which was the most abundant compound (55-70% of C), increased with depth across these sites, whereas other C compounds like carbohydrates did not vary with depth. These results suggest that there is no preferential decomposition of carbohydrates, but preferential retention of lignin. Stable isotope signatures of respiration products indicated that hydrogenotrophic rather than acetoclastic
30 methanogenesis was the dominant production pathway of CH₄ throughout the peat profile. These results show that deep C in tropical peatlands does not contribute greatly to surface fluxes of carbon dioxide, with compounds like lignin preferentially retained. This protection of deep C helps explain how peatland C is retained over thousands of years, and points to the vulnerability of this C should anaerobic conditions in these wet ecosystems change.

1 Introduction

35 Climate change is expected to disturb hydrological cycles in the tropics, with changes in rainfall regimes already observed for many tropical regions (Kharin et al. 2007, Feng et al. 2013, Magrin et al. 2014, Duffy et al. 2015, Chadwick et al. 2016, Barkhordarian et al. 2019). Changes in rainfall are of particular relevance to the storage of the 70 – 130 Gt of organic carbon (OC) stored in tropical peatland soils under anaerobic conditions, which could be under threat of rapid mineralization if rainfall declines and aerobic conditions emerge (Girkin et al., 2022; Loisel et al., 2021). Tropical peatlands store the largest pool of
40 vulnerable and irrecoverable C of any ecosystem type, and this pool is sequestered over thousands of years (Goldstein et al., 2020; Noon et al., 2021). Despite their importance, tropical peatlands are logistically challenging environments to work in and are understudied compared to their northern counterparts, making tropical peatlands underrepresented in global C inventories (Ribeiro et al., 2021).

Peatlands sequester C as they build vertically with the oldest deposits at the base and less decomposed younger material
45 accumulating at the surface (Clymo et al., 1998; Ingram, 1987). Despite temperatures ideal for microbial activity, the buildup of organic matter is possible because rates of primary production in the tropics exceed decomposition rates, which are low because peatland water tables are high (Nottingham et al., 2019; Page et al., 2011). Thus, deep peat is comprised of minimally processed plant material from the surface that accumulates due to anaerobic conditions, creating a globally significant buildup of C over time that could be metabolized if conditions became more favorable for decomposition (Hoyos-Santillan et al., 2019;
50 Kettridge et al., 2015; Wilson et al., 2021). However, this age-depth relationship is not as straightforward in the tropics as in northern peatlands, because tropical peatland microtopography shows higher variability due to increased vegetation diversity and size, and forest disturbance can have dramatic effects on peat accumulation patterns (Dommain et al., 2015; Girkin et al., 2019). The dominant vegetation that acts as the stabilizing structure in early peat development, as well as the vegetation that serves as the biological origin of the peat itself, is also different in northern and tropical peatlands, leading to differences in
55 peatland development, organic chemistry, and accumulation patterns between these two regions (United Nations Environment Programme et al., 2008).

Under current conditions, there is considerable variation in C emissions across tropical wetland systems (Farmer et al., 2011; Fritts, 2022), but some relationships have been generally characterized. It is mostly accepted that water table depth (Cobb et al., 2017; Hoyos-Santillan et al., 2019; Hoyt et al., 2019), temperature (Girkin et al., 2020; Hirano et al., 2009;
60 Jauhiainen et al., 2014), substrate availability, and associated links with the dominant vegetation type (Upton et al., 2018; Wright et al., 2011, 2013), are strong controls on surface emissions from tropical peatlands. Furthermore, surface vegetation plays an important role in peatland C cycling, both as the biological origin of the peat matrix, which is composed primarily of lignin rich fibrous material in woody tropical peatlands, and via labile C inputs in the form of decomposing plant tissues or root exudates (Girkin et al., 2018; Lampela et al., 2014; Osaki et al., 2021). The majority of studies conducted in tropical
65 peatlands have focused on the top 30 cm of the peat column; these depths are not only more accessible and easier to measure, but they are assumed to contribute the majority of emissions (Dhandapani et al., 2022; Jauhiainen et al., 2005; Sjögersten et al., 2011). However, it is not known if the above drivers are mainly restricted to the surface, or if these processes influence CO₂ and CH₄ production deeper within the peat profile.

In many peatlands, microbial respiration across the soil profile can be supported by multiple C sources, and it is possible to use the radiocarbon signature of C respired from peatlands to partition sources into modern/surface dissolved OC (DOC) transported down the soil profile, versus older/buried solid C (Chanton et al., 2008; Hoyos-Santillan et al., 2016). Modern DOC, derived from surface vegetation, root exudates, and other recently photosynthesized organic matter, has a signature that is enriched in $\Delta^{14}\text{C}$. The existing peat and DOC from *in situ* decomposition of that deep peat, would have depleted radiocarbon signatures compared to the modern DOC (Girkin et al., 2018; Wilson et al., 2016).

There have been several studies exploring the source of DOC used by microbes for respiration within peat soils. Most studies were from northern peatlands, and determined that respiration products were intermediate in their radiocarbon activity between newer surface DOC and older C in peat (Aravena et al., 1993; Chanton et al., 1995, 2008; Clymo et al., 1998; Corbett et al., 2013). Fewer studies have reported that respiration products are more similar to modern DOC radiocarbon signatures, demonstrating dominant use of surface DOC in deep peat gas production (Wilson et al., 2021). There is limited data from tropical peatlands, but two previous studies from the tropics found contrasting results; one found intermediate respiration products (i.e., produced by mixed sources) in a tropical peatland in Borneo (Hoyt, 2014), and another found modern, surface-derived inputs are the dominant source in sites across the Pastaza-Marañon basin in Peru (Hoyt et al., 2020). Potential explanations for this variable source contribution in tropical peatlands include differences in hydrology across sites, as well as the difference in dominant vegetation across the tropics. Biological origin can influence the chemistry and bioavailability of both modern DOC inputs and the resulting older peat (Dhandapani et al., 2023; Gandois et al., 2014), which could contribute to the different results reported for these two tropical peatlands with distinct surface vegetation.

Methanogenesis is an important pathway of decomposition in wetland systems. Acetoclastic methanogenesis is associated with acetate fermentation and the production of CH_4 from relatively labile organic compounds, while hydrogenotrophic methanogenesis is associated with CO_2 reduction, and can be supplied by the decomposition of more complex organic matter, with this second pathway less energetically favourable to microbes (Kotsyurbenko et al., 2004; Sugimoto and Wada, 1993). Metabolically, acetoclastic methanogenesis is more energetically favourable (i.e. more potential energy released), more efficient in CH_4 production, and generally results in higher rates of CH_4 production compared to hydrogenotrophic methanogenesis (Kotsyurbenko et al., 2004; Liebner et al., 2015). Shifts in CH_4 production pathways between acetoclastic methanogenesis and hydrogenotrophic methanogenesis occur depending on substrate availability, with acetoclastic favoured if fermentation products are available, as have been seen with depth in northern wetlands (Chanton et al., 2008; Corbett et al., 2013; Hornibrook et al., 2000). Changes in the availability of labile materials throughout the peat profile, even at depths of 2 meters, may be crucial not only for supplying the C substrate for CO_2 and CH_4 production, but also for influencing the mechanisms and quantities of CH_4 generated (Moore et al., 2013; Sun et al., 2012).

This study explored sources of soil surface C emissions, CH_4 production pathways, and organic carbon chemistry of peat in three sites in a Neotropical peatland in Panama. Previous work suggested that subsurface peat may contribute substantially to net CO_2 and CH_4 flux from this peatland, but the source of C for these emissions was unclear (Wright et al., 2011). We used a combination of stable and radioisotope signatures of CO_2 and CH_4 , and ^{13}C solid state nuclear magnetic

resonance spectroscopy (^{13}C -NMR) characterization of peat soils, to identify the sources of the C gases produced in subsurface (>30 cm) peat. We hypothesized that: H1) Surface-derived DOC is the primary C source for microbial respiration products at
105 depth, where solid peat is more chemically complex and protected against decomposition. For this hypothesis, we predicted that deep solid peat would have a higher decomposition index compared with surface peat. H2) Hydrogenotrophic methanogenesis is the dominant CH_4 production pathway at depth, resulting from decomposition of complex organic matter, rather than fermentation of more simple C compounds, which would support acetoclastic methanogenesis (Fig 1). We report and discuss radiocarbon analyses of subsurface DOC, CH_4 , and CO_2 as well as peat biomolecular characterization using solid
110 state ^{13}C -NMR spectroscopy in a tropical peatland.

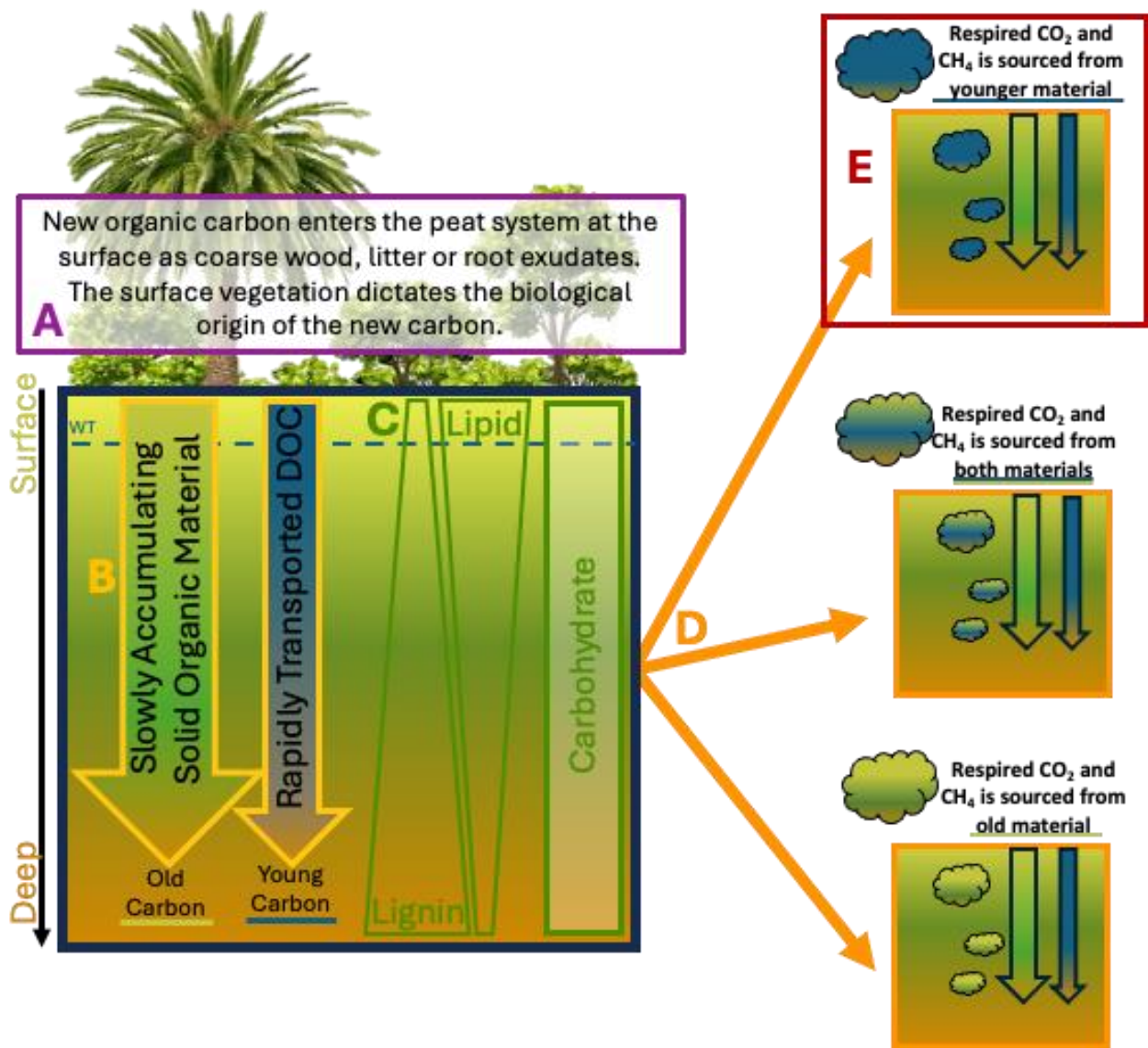


Figure 1: Schematic illustrating our conceptual understanding of the tropical peat carbon cycle. **A)** Surface vegetation acts as the primary source of new organic material entering the peat system. Key contributors include dead plant matter and root exudates, and plant species influence the organic chemistry of these C inputs to soils. **B)** Slow accumulation of solid peat matter (green) contrasts the rapid fluxes of fresh, modern dissolved organic carbon (DOC) from the surface (blue). **C)** As bulk peat accumulates over time, decomposition impacts biochemical characteristics of solid peat down the soil profile through preferential preservation of lignin and loss of lipids, while carbohydrate content remains constant. **D)** Alternative scenarios are shown for gases produced within the peat soil, which exhibit carbon isotopic signatures that reflect the dominant source material or a combination of both sources. Both organic inputs can contribute to gas production—either from a single source (top orange box and bottom orange box) or a mix of both (middle orange box). **E)** The results of this study indicate that the top scenario is most likely for these sites, with younger DOC fueling belowground respiration and methanogenesis.

2 Methods

2.1 Field Site Description

115 The Bocas del Toro Province on the Caribbean coast of Panama is home to San San Pond Sak which was designated
a Ramsar Wetland of International Importance in 1993 (site #611), which highlights the global significance of this wetland.
This site includes the 80 km² Changuinola peat deposit, an ombrotrophic domed peatland located southeast of the Changuinola
River (Fig. 2). Located 10 km east from the peatland is the town of Bocas del Toro, Isla Colón, where the average annual
rainfall and temperature are 4000 mm and 30°C respectively (Isla Colón, STRI Environmental Monitoring Station). There is
continuous rainfall throughout the year with no pronounced dry season, although there are two distinct periods of lower rainfall
120 (February–April and September–October). The water table was consistently at the surface of the peatland throughout the
sampling period, but has been reported to fluctuate from 20 cm above to 40 cm below the peat surface during high or low
rainfall (Hoyos-Santillan, 2014). Mean peat temperature 10 cm below the surface is 25 °C and shows little intra-annual
variation (Wright et al., 2011). The oldest deposits in the peatland are in the centre of the dome, are estimated to have been
formed 4000–4500 years ago, and are roughly 8 m deep (Phillips et al., 1997).

125 The Changuinola peat deposit developed from *Raphia taedigera* palm swamp, unlike southeast Asia coastal peatlands
that developed from sediment trapping mangrove stands (Anderson and Muller, 1975; Phillips et al., 1997). The vegetation
communities that formed the Changuinola peat deposits have shifted spatially over time, reflecting variations in environmental
conditions, and resulting in spatial heterogeneities in C inputs across the peatland (Cohen et al., 1989; Phillips and Bustin,
1996). At present, there are seven distinct phasic plant communities that form concentric rings within the peat dome. From the
130 periphery and moving to the interior they are as follows: (i) *Rhizophora mangle* mangrove swamp, (ii) mixed back mangrove
swamp, (iii) *Raphia taedigera* palm swamp, (iv) mixed forest swamp, (v) stunted *Camposperma panamensis* forest swamp,
(vi) sawgrass/stunted forest swamp and (vii) *Myrica-Cyrilla* bog-plain (Phillips et al., 1997). Previous work showed that
nutrient content in the peat was generally higher near the edge (1200 µg-phosphorus (P)g⁻¹, 27mg-nitrogen (N)g⁻¹) and lower
in the interior of the peatland (377 µg-Pg⁻¹, 22mg-Ng⁻¹) (Sjögersten et al., 2011; Troxler, 2007; Troxler et al., 2012).

For this study we selected sites in three of the representative plant communities, with dominant vegetation and nutrient patterns described previously. These include Outer (*Raphia taedigera* palm swamp), Intermediate (mixed forest swamp), and Inner (stunted *Camposperma panamensis* forest swamp) peatland sites (Fig. 2). Previous studies conducted within the

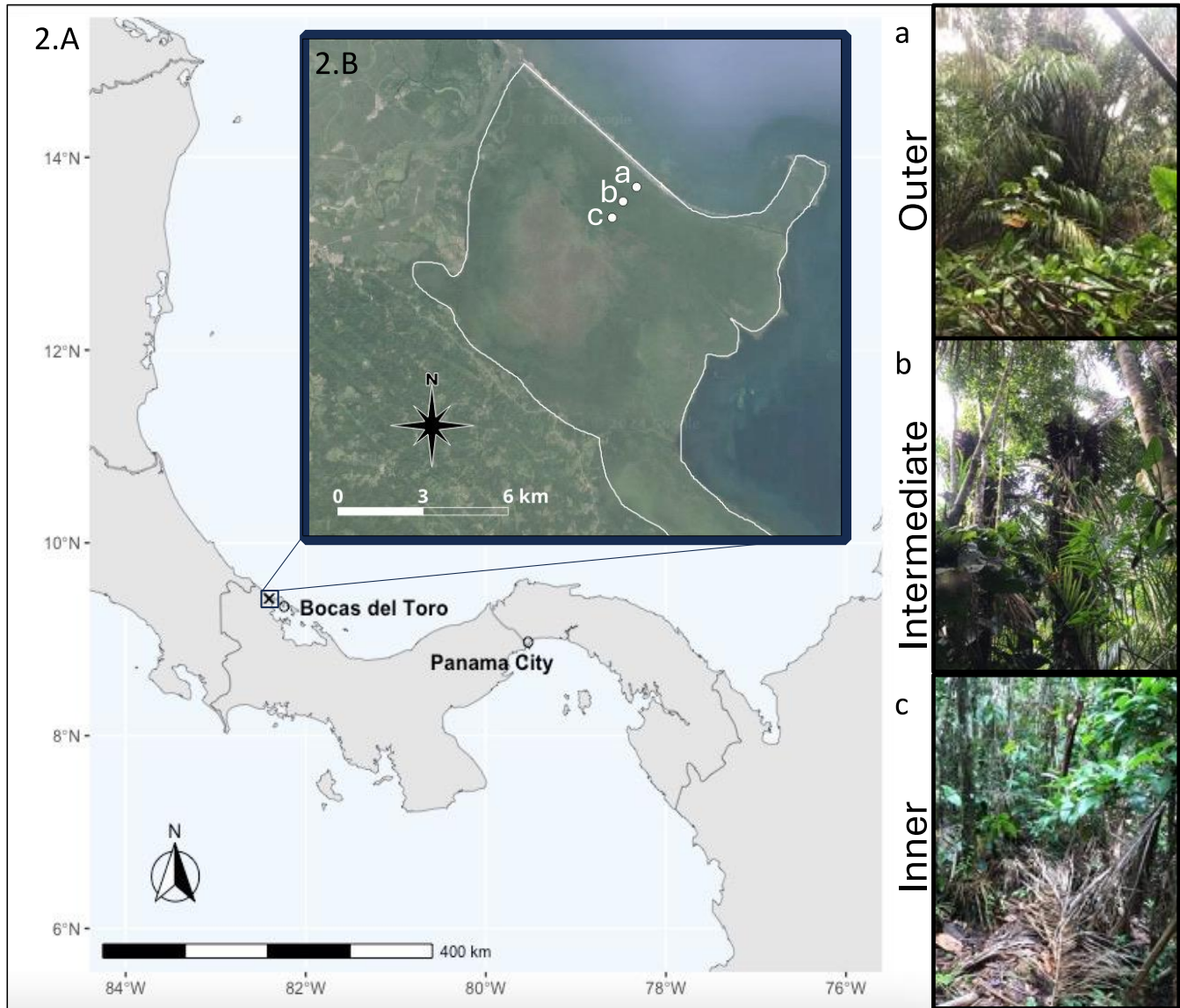


Figure 2: Map of sites included in this study from the Changuinola peat deposit. A. Location of study site identified by square in relation to the city of Bocas Del Toro and Panama City. **B.** Inset showing the location of the sites along the transect. The sites follow a vegetation gradient with a) the outer site closest to the channel, *Raphia taedigera* palm swamp b) the intermediate site mixed forest swamp and c) the inner site closest to the centre of the peatland composed of stunted *Camposperma panamensis* forest swamp. The sites follow a nutrient gradient, with nutrient content decreasing from the outer site to the inner site.

Changuinola deposit have reported differences in peat properties, root exudate characteristics, and *ex situ* experimental response in lab studies tied to vegetation community. Previously reported surface and shallow peat (<30 cm) CO₂ flux rates

140 for the outer and inner sites used here varied from 320-500 mg CO₂ m⁻² hr⁻¹ with no significant variation between sites (Wright
et al., 2011), and subsurface peat (below 30 cm) appeared to have similar carbohydrate to aromatic C ratios at the surface
(Upton et al., 2018).

2.2 Sample Collection

Bulk peat, pore water samples, and greenhouse gases (CO₂ and CH₄) were collected in October of 2019. We sampled
145 from 30 cm to basal depths that were identified by a marine clay boundary at the base of the peat, and did not sample surface
samples (0–30 cm) that might have stronger surface vegetation influence on peat chemistry compared to deeper layers that are
further along in the decomposition process (Barreto and Lindo, 2020). This study aimed to compare bulk peat and pore water
components of deep peat with gas produced at the same depth, and for that reason only those deeper samples were collected.
Peat cores were collected using a 5.2 cm diameter and 51 cm long peat sampler (Eijkelkamp, Product code 04.09). Bulk peat,
150 pore water samples, and greenhouse gases (CO₂ and CH₄) were collected in October of 2019 from depths of 30 ± 5 and 60 ±
5 cm, as well as 100 ± 5, 200 ± 5, 300 ± 5, and 400 ± 5 cm depending on total peat depth at each site. Porewater was collected
using a peristaltic pump with Teflon tubing from 1.25 cm diameter PVC pipe piezometers to measure DOC from the same
depths as the peat collection. Porewater was filtered with 45 μm particle retention using plastic syringes fitted with stopcocks
and filters and deposited into 50 ml falcon tubes for transport. Following collection, peat cores were subsampled to coordinate
155 with gas well depths and sealed in plastic bags to avoid oxidation during transport to the Smithsonian Tropical Research
Institute soils lab in Panama City, Panama.

Diffusion gas wells were deployed at the intermediate and outer site at the same depths as pore water and peat
collection to ensure robust comparison between the two source materials (bulk peat and DOC) and respiration products. There
was insufficient time to include the inner site in gas collection at time of sampling. These diffusion wells consisted of PVC
160 pipe with mesh coverings positioned within the peat to allow water to be sampled from the desired depth without contamination
of bulk peat or water pulled from other depths. Water was taken from the desired depth using a peristaltic pump and cycled
into a 1L glass container. The headspace within the glass container was allowed to equilibrate over several hours while the
water was pumped through the container at a rate of 1.5–1.8 L/min. Air samples from the equilibrated headspace were taken
using a syringe fitted with a stopcock and needle and deposited into evacuated 125 ml serum bottles fitted with heavy butyl
165 rubber septa.

2.3 Elemental and Isotopic Analyses

Elemental composition of solid homogenized airdried peat was analysed using an elemental analyser 205 (CHNOS)
coupled to an IsoPrime 100 isotope ratio mass spectrometer at the Center for Stable Isotope Biogeochemistry (CSIB) 206 at
the University of California, Berkeley. This analysis produced measurements for percent C and N, δ¹³C, and δ¹⁵N. The ash
170 content of bulk peat was determined by ignition of aliquots (~1.0 g) at 460°C for 5 hr.

Sample preparation and analysis for $\Delta^{14}\text{C}$ was completed at the Center for Accelerator Mass Spectrometry (CAMS) at Lawrence Livermore National Laboratory. To ensure that peat samples were handled appropriately for both biogeochemistry and chronology, following homogenization with a ball and mill grinder we measured two subsamples; one that underwent acid-base-acid (ABA) pre-treatment to remove possible interfering carbonates and modern C derived humic acids, and a second with no pre-treatment (Norris et al., 2020). Samples were immersed in 1N hydrochloric acid (HCL) to remove carbohydrates. Humic acids were then removed from the sample with 0.25M sodium hydroxide (NaOH) and treated with a 1N HCL immersion before they were rinsed with deionized water until neutral. The pre-treated samples were then placed on a heating block until dried. The two sets of peat samples had identical $\Delta^{14}\text{C}$ results and the no pre-treatment values were used in this study (Table A1). The porewater DOC samples were acidified with 1N HCl at 70°C to remove dissolved inorganic C and freeze dried. Both sets of peat samples and the residual DOC were loaded into quartz tubes with excess CuO and combusted at 900°C to ensure complete combustion to CO_2 .

Gas samples for CH_4 and CO_2 were extracted following the protocol outlined by McNicol et al (2020). For $^{14}\text{CO}_2$ samples, a series of cryogenic traps were used to purify and isolate the CO_2 . For $^{14}\text{CH}_4$ samples, the mixed composition field samples were cryogenically purified to remove water and CO_2 , and the remaining CH_4 was converted to CO_2 by combustion (Petrenko et al., 2008). Resulting CO_2 from samples was split to measure both a $\delta^{13}\text{C}$ and $\Delta^{14}\text{C}$. Extracted CO_2 and CH_4 were analysed for $\Delta^{14}\text{C}$ and $\delta^{13}\text{C}$ when possible, but some sample masses were too small for both analyses (minimum 20 ug C needed for $\Delta^{14}\text{C}$ analysis and for the purpose of this study, we prioritized measurements for $\Delta^{14}\text{C}$). The $\delta^{13}\text{C}$ values were analysed at the Stable Isotope Geosciences Facility at Texas A&M University on a Thermo Scientific MAT 253 Dual Inlet Stable Isotope Ratio Mass Spectrometer. To obtain a $\Delta^{14}\text{C}$ measurement, the CO_2 was reduced to graphite onto Fe powder in the presence of H_2 (Vogel et al., 1984) and analysed on the HVEC 10 MV Model FN Tandem Van de Graaff Accelerator or the NEC 1 MV Pelletron Tandem Accelerator at CAMS (Broek et al., 2021). $\Delta^{14}\text{C}$ values are reported as $\Delta^{14}\text{C}$ (‰) corrected to the year of measurement (2019) and for mass-dependent fractionation using $\delta^{13}\text{C}$ values, and age is reported in years before present (yBP) within two standard deviations using the Libby half-life of 5568 years (Stuiver and Polach, 1977). Age-depth models were generated for each site in R v.4.2.2 (The R Foundation for Statistical Computing, 2022) using the “rbacon” package v2.3.9.1. BACON (Bayesian accumulation), which is based on Bayesian theory, and simulates the sediment deposition process while accounting for both variable deposition rates and spatial autocorrelation of deposition from one layer to another within the core (Blaauw and Christen, 2011) (Blaauw and Christen, 2011). Long-term peat accumulation rates were estimated by fitting linear regressions to age-depth model outputs. The calibrated ages showed timing of peat development and accumulation between the three sites, and the conventional radiocarbon values were used to compare and identify the sources of material used to generate CO_2 and CH_4 at depth.

Differences in stable isotopic ($\delta^{13}\text{C}$) composition between $\delta^{13}\text{CO}_2$ and $\delta^{13}\text{CH}_4$ can identify the dominant pathway that produces methane, because hydrogenotrophic methanogenesis fractionates against heavy C isotopes more than acetoclastic methanogenesis (Wilson et al., 2016). Based on the measured stable carbon isotope signatures of CH_4 ($\delta^{13}\text{C}\text{-CH}_4$) and CO_2 ($\delta^{13}\text{C}\text{-CO}_2$) in dissolved gas in peat pore water, we calculated the apparent carbon isotope fractionation (α_{app}) for this

205 methanogenic process according to formula: $\alpha = (\delta^{13}\text{CO}_2 + 1000) / (\delta^{13}\text{CH}_4 + 1000)$. Values of $\alpha_{\text{app}} = [(\delta^{13}\text{CO}_2 + 1000) / (\delta^{13}\text{CH}_4 + 1000)]$ that are greater than 1.065 are characteristic of environments dominated by hydrogenotrophic methanogenesis, while values lower than 1.055 are characteristic of environments dominated by acetoclastic methanogenesis (Zhang et al., 2019).

2.4 ^{13}C -NMR Spectroscopy and Mixing Model

210 Solid State ^{13}C NMR spectra of untreated peat samples were obtained at the Pacific Northwest National Laboratory in Washington state at the Environmental Molecular Science Laboratory facility using cross-polarization under magic angle spinning conditions (CP/MAS) with a Varian Direct Drive NMR spectrometer equipped with a Varian 4-mm probe. These bulk peat samples were free of charcoal. Approximately 30 mg of peat were packed in 4 mm zirconia rotors sealed with Kel-F caps. The CP spectra were acquired after 14k scans with a MAS rate of 14 kHz resulting in no interference from sidebands as they were outside the range of the spectrum, and a ramp-CP contact time on proton of 1 ms and a 1 or 2 s recycle delay
215 depending on the sample with 62.5 kHz tppm proton decoupling (Aliev, 2020). The one-dimensional ^1H NMR spectra of all samples were processed and analysed relative to the external standard adamantane. All spectra were corrected against a KBr background, and signals arising from C in the NMR probe and rotor were accounted for by subtracting the spectra of an empty rotor from the sample. Spectra were digitally processed with exponential apodization (100 Hz line broadening with the first point set to 0.50), phase correction, and baseline correction using a Bernstein polynomial fit with Mnova software (v. 14.3.3;
220 Mestrelab Research). Peak areas were integrated within seven chemical shift regions for input to the molecular mixing model corresponding to: alkyl C (0–45 ppm), N-alkyl/methoxyl C (45–60 ppm), O-alkyl C (60–95 ppm), di-O-alkyl (95–110), aromatic C (110–145 ppm), phenolic C (145–165 ppm), and carboxyl C (165–215 ppm).

We used a mixing model which incorporates six components to describe the molecular composition of samples based on ^{13}C NMR outputs (Baldock et al., 2004). This peatland soil has no visual evidence of char, so that component was removed
225 from the model. The five remaining components (carbohydrate, protein, lipid, lignin, and carbonyl) have each been assigned a discrete percent of different regions of the ^{13}C NMR signal intensity based on knowledge of molar elemental contents and C content of terrestrial soil ecosystems. The measured C:N ratio of each sample was used to constrain the protein concentration of each ^{13}C NMR spectrum in the molecular mixing model. The optimisation process of the molecular mixing model compares fits for all five biomolecules to models eliminating one, two, and three components; in all cases the model fit was best when
230 all five components were included in the model (sum of squares of deviation < 6%). The mixing model outputs are available in Table A2.

2.6 Statistics

We assessed our data at two scales: 1) among-site comparisons of the three sites, considering overall differences in peat characteristics and isotopic signatures and 2) peatland-wide patterns in soil profile characteristics and relationships among
235 peat chemistry and isotopic signatures. Relationships between peat physical properties (C and N concentrations, C:N, $\delta^{13}\text{C}$, $\delta^{15}\text{N}$, and radiocarbon) and the five biomolecules identified with the molecular mixing model were assessed using Pearson

correlation analysis. We also conducted separate analyses of the ^{13}C -NMR data using raw data for spectral regions. The three sites were pooled to get peatland scale relationships between the peat physical properties and the five biomolecules versus depth. Due to the limited size of this dataset, the spearman method was used to measure covariance and the coefficients are reported in the full correlation matrix results, including r^2 values and significance, in supplementary materials (Fig. A3 & A4). We assessed differences among the three sites using Principal Component Analysis (PCA) based on all factors included in the correlation matrices (all peat physical properties, chemistry, and isotopes for each site). Significant trends in biomolecule abundance across depth were identified by linear regression. To identify differences between mean radiocarbon values of the sources and respiration products we utilized two-sample t-tests. Bulk peat and gas products were determined by Welch two-sample t-test to account for lack of homogeneity of variance, and differences between mean radiocarbon values of DOC and gas products were assessed by student two sample t-test. All relationships explored were considered significant at the 0.1 alpha level. Statistical analyses were conducted in R v.4.2.2 (The R Foundation for Statistical Computing, 2022). Reported means in the text are shown with standard errors in parentheses.

3 Results

3.1 Isotopic composition of source material and respiration products

Across all sites and depths, radiocarbon signatures of dissolved CH_4 and CO_2 were relatively modern (i.e., ^{14}C -enriched) relative to peat soil, and had similar $\Delta^{14}\text{C}$ values to DOC from peat pore water water, indicating the dominant contribution of modern C for soil respiration and methane production (Fig 3). Overall, the respiration products had statistically similar radiocarbon values to the DOC ($t(23)=0.534$ $p= 0.60$) compared to the bulk peat ($t(16)=|8.67|$, $p= <0.05$) (Table S3). The radiocarbon values for the bulk peat with depth are consistent with accumulation of C over time. The calibrated basal ages

for deep peat soil from outer, intermediate, and inner sites were 1215 ± 35 , 1060 ± 30 , and 1750 ± 35 cal yrBP respectively, indicating the age of the peatland.

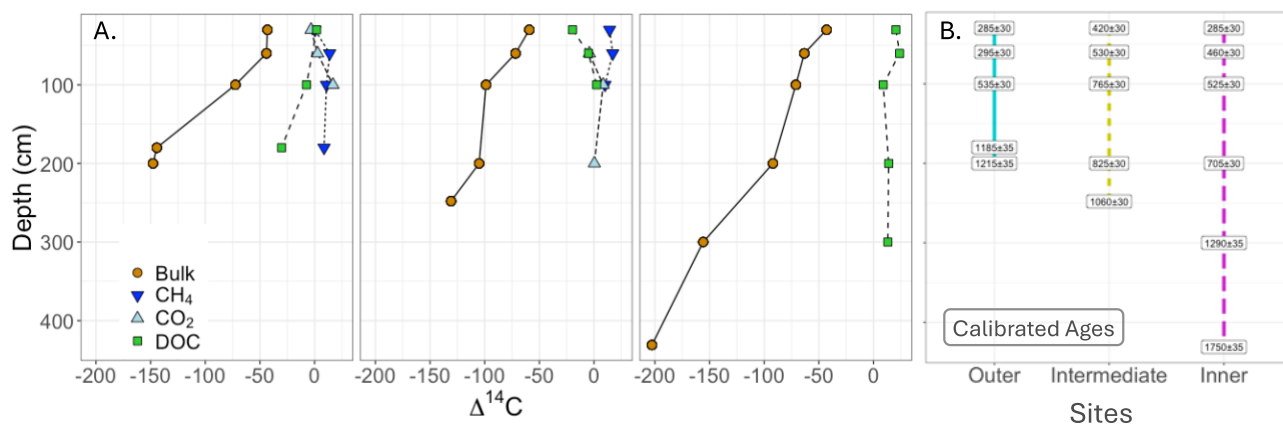


Figure 3. Isotopic composition of respiration products and substrates. Bulk peat, DOC, and respiration products (CH_4 = methane, CO_2 = carbon dioxide) plotted by depth for the three sites: **A)** outer, **B)** intermediate and **C)** inner peatland sites. Brown circles and solid lines represent bulk peat, and green squares with dashed lines represent DOC, which are the two measured sources for gas production. The gas products are denoted by inverted dark blue triangles and dotted lines for methane, and light blue triangles and dashed lines for dissolved carbon dioxide. Note the age difference between solid peat and all DOC and gas values; this offset suggests that gas production is driven by modern DOC throughout the peat profile. **D.** Calibrated ages for all bulk peat measured in yBP within instrument error for the outer (blue), intermediate (yellow), and inner (pink) sites are shown.

3.2 Peat Properties and Chemistry

The percent OC across the sites ranged from 40–55% from the surface to basal depths, with lower OC content and higher ash content at depth, likely reflecting the incorporation of underlying mineral sediments into base layers. The negative correlations between both OC and N concentrations with depth were not significant (Figs. 4A, 4B and 4C), however the negative correlations between ash content and depth ($r(16) = -0.62$, $p \leq 0.1$) and age and depth ($r(16) = -0.93$, $p \leq 0.1$, Fig. 4) were strongly significant (Fig. A3). Bulk peat stable isotopes, $\delta^{13}\text{C}$ and $\delta^{15}\text{N}$, showed no strong relationship with depth or site (Figs 4D and 4E). Linear slopes across the age-depth profiles suggested consistent peat accumulation rates across the peatland over time (Fig. 4F). Estimates of long-term peat accumulation rates were calculated using the calibrated ages, and were 0.192 cm yr^{-1} , 0.473 cm yr^{-1} , and 0.275 cm yr^{-1} for the outer, intermediate, and inner sites respectfully. Example spectra can be seen in appendix figure A1. The ^{13}C -NMR molecular mixing model results showed that depth was positively correlated with lignin ($r(16) = 0.70$, $p \leq 0.1$) and negatively correlated with lipid abundance ($r(16) = -0.54$, $p \leq 0.1$) (Figs 5A–C, and Fig A4). To further explore patterns in peat chemistry across depth, we pooled the three sites for linear regression. We found significant decreases in lipid abundance ($R^2 = 0.25$, $F(1,14) = 5.88$, $p < 0.029$) and increases in lignin abundance ($R^2 = 0.46$, $F(1,14) = 13.7$, $p < 0.002$) with increasing depth (Fig A6).

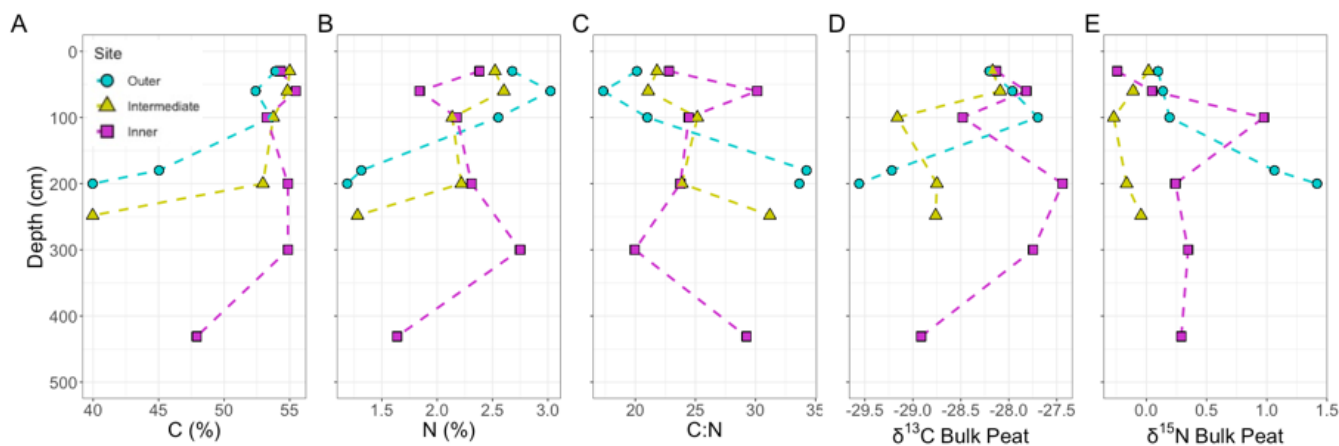


Figure 4. Bulk Peat Properties and Characteristics. Depth profiles for A. percent carbon, B. percent nitrogen, C. the ratio of carbon to nitrogen, D. stable carbon isotope, E. stable nitrogen isotope, and E. calibrated age for layers measured for the three sites. Sites are indicated by colour and shape with blue circles indicating the outer site, yellow triangles the intermediate site, and pink squares the inner site. Statistical correlations with depth were seen between age (yBP).

Compared to the other four molecular components (protein, lipid, carbonyl, and carbohydrate), lignin was the most abundant biomarker making up an average of $64\% \pm 1.1$ of peat organic matter across depths and sites (Fig 5.D). Carbohydrate was the second most abundant compound and averaged $17\% \pm 0.2$ across samples. There was almost no carbonyl-C present (all sites averaged $< 2\%$), except for deep peat at the outer site and 60 and 200 cm layers of the inner site, which had $0.4\% \pm 0.9$ and $2\% \pm 2$ carbonyl-C respectively (Figs 5A and 5C). Overall, the organic chemistry of peat was very similar across the sites, and the main patterns that emerged were with depth.

Our PCA indicated differences in peat properties among the three sites. The scores and loadings of the first and second principal components accounted for the majority of variance (74%) with the first principal component accounting for 54.93% (Fig 6A). Separation along the first principal component axis showed stratigraphic effects related to depth and peat accumulation over time, with strong separation between the 30 and 60 cm layers versus the underlying peat (symbols, Fig. 6A). The clustering of the 30 and 60 cm peat layers on PC1 can be attributed to strong axis loadings by OC, lipid, alkyl-C, and protein contributions to soil OC (Fig 6B, Table A2). By contrast, PC2 was mainly described by site differences, with the inner site most distinct (Fig 6A). This separation appeared to be tied to loadings on this axis by carbonyl, which was different among the sites (Fig 6B, Table A2, Table A4).

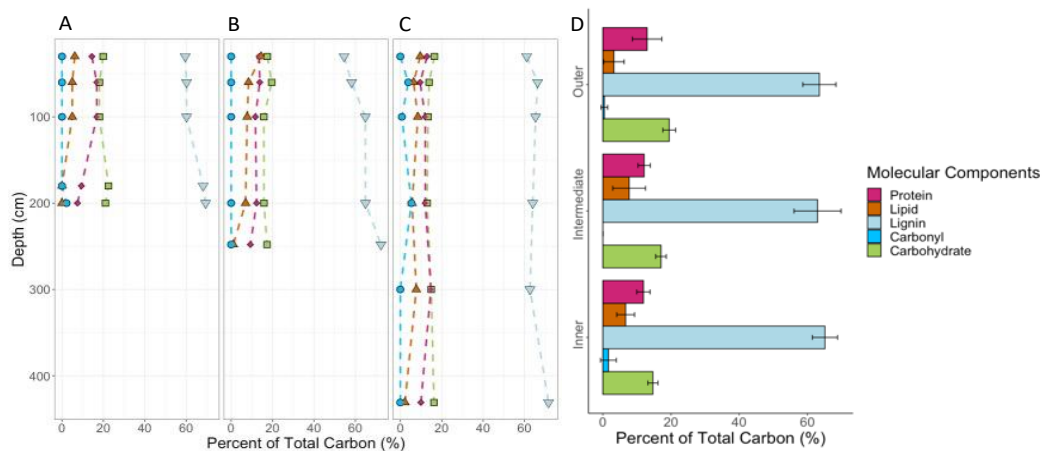


Figure 5. Proportion of total organic C attributed to each molecular component across sites and depths. Mixing model results are shown, indicating little change in the five molecular components with depth for the **A)** outer, **B)** intermediate, and **C)** inner sites. Colors and symbols represent the molecular components: proteins = pink diamonds, lipids = orange triangles, lignin = light blue inverted triangles, carbonyl = blue circles, and carbohydrates = green squares. **D)** Average proportions of total organic C attributed to each molecular component across sites are shown with standard error.

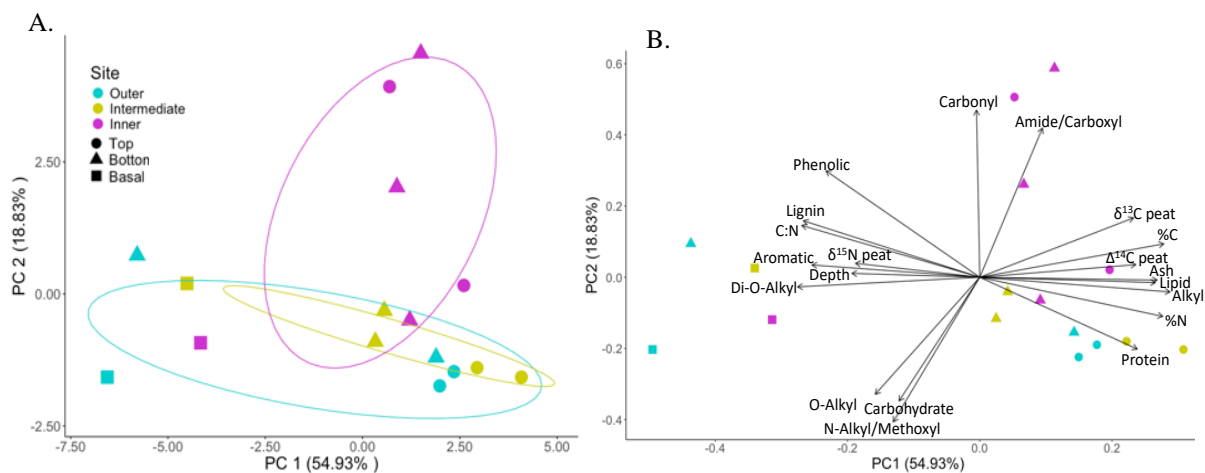


Figure 6. Clusters by site and relative factor loadings are shown for the PCA. **7A** shown clustering by site for the outer (blue), intermediate (yellow), and inner (pink) sites, with depths indicated by shape: top (30-60 cm) as circles, deep (>1 m) as triangles, and the three basal depths as squares (basal depths; Outer 200 cm, Intermediate 248 cm, and Inner 431cm). Combined PC1 and PC2 account for 74% of variance. Separation on PC1 is primarily by depth, while separation on PC2 is primarily by site (A), with factors contributing to these separations shown (B).

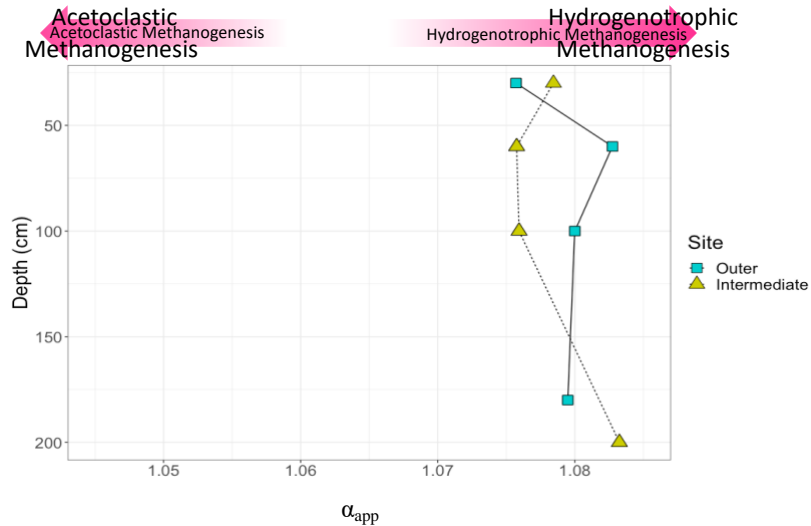


Figure 7. Differences in stable C isotopic composition between DIC and CH₄. Calculated estimates of apparent fractionation factor (α_{app}) in methane production across depths are shown for gas collected from the outer (blue squares) and intermediate (green triangles) sites. The samples from the inner site did not have sufficient amounts of C for this analysis. The x-axis shows little variation in α_{app} between sites and soil depths. Values of α_{app} higher than 1.065 are characteristic of environments dominated by hydrogenotrophic methanogenesis, while a value lower than 1.055 would be characteristic of acetoclastic methanogenesis (Corbett et al., 2013).

3.3 Using $\delta^{13}\text{C}$ to identify CH₄ Production Pathway

The α_{app} values for methanogenesis pathway overlap between the outer and intermediate sites and averaged 1.078 (+/- 0.003) (Fig. 7). The data indicate no shift in α_{app} with depth throughout the peat profile. The α_{app} values indicate hydrogenotrophic methanogenesis as the dominant production pathway across all depths measured at the outer and intermediate sites.

4. Discussion

4.1 Source

The Changuinola peatland is important as an internationally protected wetland and is an example of a pristine undisturbed functioning tropical peatland. This is supported by the age-depth profiles that showed continuous undisturbed peat accumulation over the past 1060 to 1750 years. Peatland soils had similar OC and N concentrations and C:N ratios compared to other ombrotrophic peat domes across the tropics (Beilman et al., 2019; Dargie et al., 2017; Lahteenoja et al., 2012; Omar et al., 2022). Our data contribute a novel characterization of the organic components of solid and dissolved C in tropical peats, and the likely contributions of these to CO₂ and CH₄ fluxes. Across all sites and depths, DOC had modern (enriched) radiocarbon signatures compared to the bulk peat, indicating it is largely derived from recent photosynthate. In contrast to the

DOC originating from newer surface organic material, the solid peat becomes progressively older with depth, having accumulated over long timeframes. Our data notably show an age similarity between respiration products and modern DOC radiocarbon values across depths. This strongly suggests vertical transport of modern C from the surface to deeper soil layers, which is then used in microbial metabolism. It is important to note that root exudation and turnover could also contribute modern DOC at depth, modern CO₂ values at depth could reflect root respiration, and modern root respired CO₂ could also serve as a C source for methane production throughout the peat profile. The modern radiocarbon signature of methane at depth suggests that microbial metabolism is also dependent on modern C inputs, and that older, buried peat C is not contributing substantially to respiration. Other tropical peatlands have showed mixed patterns of substrate age for respiration products. Similar patterns have been reported in other tropical peatlands, where modern DOC appears to be the main substrate for deep soil microbial respiration (Hoyt et al., 2020). In contrast one peatland in Borneo reported respiration products from mixed sources (Hoyt, 2014). These contrasting results suggest that there is need to explore more tropical peatland sites to characterize substrate use by microbial metabolism in the tropics. One likely reason that deeper solid peat is not utilized as much in microbial metabolism as more modern DOC is the organic chemistry of deep peat. Specifically, deeper peat had higher lignin content compared with surface peat.

4.2 Peat Chemistry and Stabilization

The dominant biomolecule making up this peat OC was lignin, which generally represented >60% of the OC in our samples. Despite the lack of a depth difference in the aromaticity index, we saw an accumulation of lignin with depth, indicating preferential preservation of this biomolecule and microbial discrimination against its decomposition through time. The waterlogged conditions in tropical peatlands can particularly reduce the decomposition of lignin by inhibiting ligninolytic microbes (Hoyos-Santillan et al., 2015; Thormann, 2006). This selective preservation of lignin has been reported for this wetland (Hoyos-Santillan et al., 2016) and other tropical peatlands (Gandois et al., 2014) previously, and supports a paradigm of selective preservation of aromatic compounds under anaerobic conditions. Coarse woody material from fallen trees, branches, and dead roots contribute a large yet relatively sporadic portion of OC inputs to tropical peat, in addition to the more constant inputs from leaf litter and fine root turnover (Hodgkins et al., 2018), and our data together with the previous studies indicate that this large-scale tree mortality and branch shedding is crucial for peat OC accumulation.

There was little change in the carbohydrate portion of peat OC with depth, although carbohydrates typically represent the most labile compounds in plant tissues for decomposition (Bader et al., 2018). That is, available carbohydrates were probably quickly decomposed at the surface, with remaining carbohydrates subsequently preserved as peat accumulated. Interestingly, there was a significant decline in lipids with depth, even though other tropical and temperate forest studies have indicated preferential preservation of lipids in upland soils (Cusack et al., 2018; Jastrow et al., 2007; Wiesenberger et al., 2010). Our data could indicate several non-exclusive patterns, including that under anaerobic conditions, lipids are decomposed more than other compounds, and/or microbial biomass production of lipids declines, and/or there were changes in the lipid content of microbial and plant C inputs to soils over time.

335 Surprisingly, we did not see strong differences in peatland organic chemistry among the three sites, even though plant cover did change. Our outer site is closest to the edge of the peatland in an area of the peatland that is dominated by *Raphia taedigera* palm swamp and has relatively high nutrient availability, while the intermediate site is dominated by mixed forest swamp species, and the inner site closest to the centre of the peatland is dominated by stunted *Camposperma panamensis* forest and has relatively low nutrient availability (Phillips and Bustin, 1996; Sjögersten et al., 2011; Troxler, 2007).

340 Based on the $\Delta^{14}\text{C}$ age of peat collected across these sites, the dome shape of the peatland has built up with older layers closer to the surface at the margins (Fig 8). This shape and accumulation pattern has been described and modelled across other tropical peat domes that have the similar ombrotrophic characteristics as Changuinola (Cobb et al., 2017, 2024). Because of the organic chemistry similarities across sites, our results suggest age was not a driver of peat chemical characteristics or properties that describe decomposability. Older peat that accumulated over 1000 years ago is closer to the surface at the margins of the peatland, and would thus be more vulnerable to changes in water table and aerobic conditions if there were changes in water table or disturbance (Dommain et al., 2011).

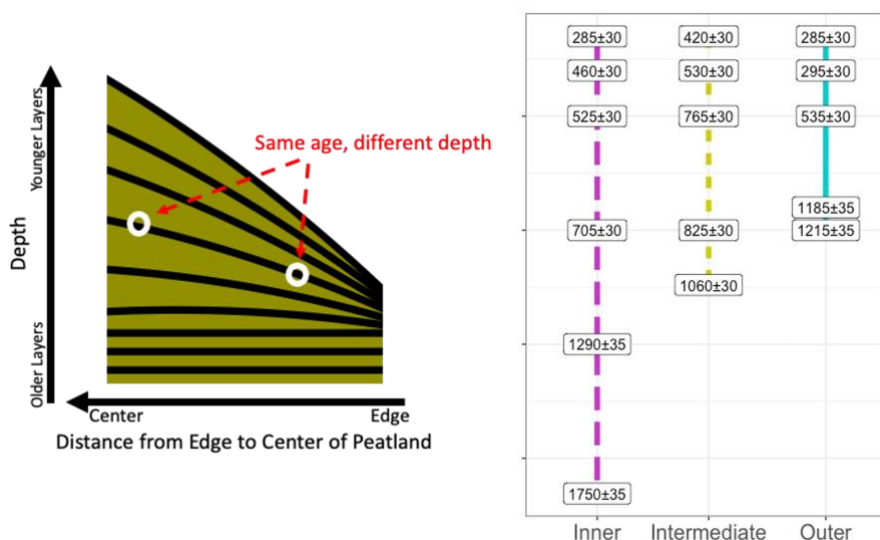


Figure 8: Schematic of peatland shape and layer accumulation pattern based on peat layer age and depth from surface. This concept was presented in model data from Cobb et al., 2017 and has been modified to create this schematic that is not to scale. Peat layers accumulate over time with the youngest layers at the surface and oldest layers at the base of the peat deposit. Based on this and ages collected from the sites within the Changuinola peat deposit, layers that correspond to the same age are located at different depths across the peat dome with older peat layers are closer to the surface at the margins.

Using $\delta^{13}\text{C}$ to understand CH_4 Production

In other studies from this peatland site, peat organic matter quality influences the CH_4 production pathway (Holmes et al., 2015). When easily degradable inputs are decomposed, acetate is produced by fermentative bacteria, promoting acetoclastic methanogenesis (Mobilian and Craft, 2022). After the labile material is depleted, the decomposition of more resistant material

350

and related CO₂ production promotes hydrogenotrophic methanogenesis (Conrad, 2020). The high α_{app} (1.078 ± 0.003) values observed here indicate that hydrogenotrophic methanogenesis was the dominant production pathway across depths. CO₂ produced in the initial steps of decomposition is a strong potential supply of CO₂ to support hydrogenotrophic methanogenesis (Gruca-Rokosz and Koszelnik, 2018; Kotsyurbenko et al., 2004).

355 Although both northern and tropical peatlands may exhibit hydrogenotrophic methanogenesis as the dominant pathway, the $\delta^{13}\text{C}\text{-CH}_4$ signature differs widely due to variations in precursor $\delta^{13}\text{C}\text{-CO}_2$, influenced by temperature, microbial activity, organic matter composition, and decomposition processes (Holmes et al., 2015). While this study does not imply that tropical peatlands function differently from temperate peatlands, these findings suggest that research in higher-latitude peatlands offers a basis to explore OC cycling in tropical peatlands. However, additional validation is needed to confirm that they operate
360 similarly. In summary, our findings indicate that these peatlands rely heavily on surface-derived DOC to support deep peat microbial respiration and methanogenesis, produce CH₄ primarily through hydrogenotrophic methanogenesis, and accumulate lignin-rich, carbon-dense peat at depth, with anaerobic conditions playing an important role in maintaining these processes.

Future Implications

Tropical peatlands, such as the Changuinola peat deposit, represent critical carbon-rich ecosystems that play a substantial
365 role in the global carbon cycle but face vulnerability under future climate scenarios. However, this carbon storage mechanism is sensitive to shifts in climate, hydrology, vegetation, and land use change. Changes in precipitation patterns and increased evapotranspiration associated with climate change could disrupt the connectivity between surface and deep peat layers, altering DOC transport and potentially increasing the exposure of preserved peat to aerobic conditions. The predominance of lignin, resistant under anoxic conditions, raises questions about its vulnerability when exposed to oxygen. If peatlands dry out, the
370 preserved OC could rapidly decompose, shifting the ecosystem from a sink to a potential carbon source, with significant greenhouse gas release (Kettridge et al., 2015; Ofiti et al., 2023).

Our study underscores the need for further research on the resilience of tropical peatlands under changing environmental conditions. Key areas for future work include examining how shifts in vegetation and surface inputs could influence OC dynamics and gas production. Variations in plant community composition and changes in nutrient status may affect DOC
375 quality and quantity, potentially altering the balance between acetoclastic and hydrogenotrophic methanogenesis pathways. Additionally, further investigation into the microbial communities driving peat decomposition and CH₄ production could yield insights into how these processes may shift with changing environmental factors.

Comparative studies between high-latitude and tropical peatlands highlight the unique characteristics of tropical systems, which are subject to faster biomass production and decomposition rates in warmer climates. Unlike high-latitude peatlands,
380 which accumulate OC slowly over millennia, tropical peatlands maintain a more dynamic OC balance. This difference suggests that tropical peatlands may be particularly vulnerable to rapid changes in hydrology and land use. Understanding how such factors interact to influence peat accumulation, organic matter preservation, and greenhouse gas flux is essential for assessing the stability of tropical peatlands in a warming world.

To fully realize the climate mitigation potential of tropical peatlands, future studies must address how these ecosystems
385 respond to both gradual and abrupt environmental changes. The development of long-term conservation and restoration
strategies will depend on our ability to anticipate the impacts of altered hydrology and vegetation composition on peatland OC
storage. Continued research into these processes is vital for informing global climate policies and ensuring the preservation of
these irreplaceable OC reservoirs.

390

Appendix A

395 Table A1: **Radiocarbon results for both untreated (No Acid-Base-Acid) and treated (Acid-Base-Acid) sets of peat samples.** Radiocarbon concentration is expressed as $\Delta^{14}\text{C}$ with instrument error.

Site	Depth (cm)	$\Delta^{14}\text{C}$ (No ABA)	\pm	$\Delta^{14}\text{C}$ (ABA)	\pm
Outer	30	-43.1	3.4	-54.9	4.1
	60	-44.0	3.4	-54.2	4.1
	100	-72.4	3.1	-77.5	4.0
	180	-147.8	3.2	-157.6	3.6
	200	-144.3	3.2	-157.8	3.6
Intermediate	30	-59.2	3.4	-59.9	4.0
	60	-71.8	3.3	-70.2	4.0
	100	-98.8	3.3	-107.5	3.8
	200	-105.1	3.2	-110.8	3.8
	248	-130.8	3.2	-141.0	3.7
Inner	30	-42.9	3.3	-45.6	4.1
	60	-63.3	3.3	-68.5	4.0
	100	-71.0	3.2	-75.9	4.0
	200	-92.0	3.3	-93.6	3.9
	300	-155.8	3.2	-155.2	3.6
	431	-202.7	3.1	-203.1	3.4

400

405

Table A2: **Mixing model outputs for all depths sampled from the three sites.** Molecular component proportion of total C measured via ^{13}C NMR described by the mixing model output as weighted percent (Wt%) developed by Baldock et al., 2004, %C measured from bulk peat combustion via elemental analyzer.

Site	Depth (cm)	Molecular Component	Wt%	%C
Inner	30	Carbohydrate	16.5	54.33
Inner	30	Protein	12.9	54.33
Inner	30	Lignin	61.0	54.33
Inner	30	Lipid	9.6	54.33
Inner	30	Carbonyl	0.0	54.33
Inner	60	Carbohydrate	13.9	55.49
Inner	60	Protein	9.6	55.49
Inner	60	Lignin	66.3	55.49
Inner	60	Lipid	6.4	55.49
Inner	60	Carbonyl	3.8	55.49
Inner	100	Carbohydrate	13.4	53.24
Inner	100	Protein	12.1	53.24
Inner	100	Lignin	65.3	53.24
Inner	100	Lipid	8.5	53.24
Inner	100	Carbonyl	0.7	53.24
Inner	200	Carbohydrate	13.0	54.87
Inner	200	Protein	12.1	54.87
Inner	200	Lignin	64.0	54.87
Inner	200	Lipid	5.7	54.87
Inner	200	Carbonyl	5.3	54.87
Inner	300	Carbohydrate	14.9	54.88
Inner	300	Protein	14.8	54.88
Inner	300	Lignin	62.6	54.88
Inner	300	Lipid	7.7	54.88

Inner	300	Carbonyl	0.0	54.88
Inner	431	Carbohydrate	16.3	47.91
Inner	431	Protein	9.9	47.91
Inner	431	Lignin	71.6	47.91
Inner	431	Lipid	2.2	47.91
Inner	431	Carbonyl	0.0	47.91
Intermediate	30	Carbohydrate	17.4	55.01
Intermediate	30	Protein	13.5	55.01
Intermediate	30	Lignin	54.5	55.01
Intermediate	30	Lipid	14.5	55.01
Intermediate	30	Carbonyl	0.0	55.01
Intermediate	60	Carbohydrate	19.6	54.84
Intermediate	60	Protein	13.8	54.84
Intermediate	60	Lignin	58.2	54.84
Intermediate	60	Lipid	8.4	54.84
Intermediate	60	Carbonyl	0.0	54.84
Intermediate	100	Carbohydrate	15.8	53.76
Intermediate	100	Protein	11.7	53.76
Intermediate	100	Lignin	64.8	53.76
Intermediate	100	Lipid	7.7	53.76
Intermediate	100	Carbonyl	0.0	53.76
Intermediate	200	Carbohydrate	15.9	52.96
Intermediate	200	Protein	12.3	52.96
Intermediate	200	Lignin	64.9	52.96
Intermediate	200	Lipid	7.0	52.96
Intermediate	200	Carbonyl	0.0	52.96
Intermediate	248	Carbohydrate	17.3	39.96

Intermediate	248	Protein	9.3	39.96
Intermediate	248	Lignin	72.4	39.96
Intermediate	248	Lipid	1.0	39.96
Intermediate	248	Carbonyl	0.0	39.96
Outer	30	Carbohydrate	19.9	53.92
Outer	30	Protein	14.4	53.92
Outer	30	Lignin	59.5	53.92
Outer	30	Lipid	6.2	53.92
Outer	30	Carbonyl	0.0	53.92
Outer	60	Carbohydrate	18.1	52.40
Outer	60	Protein	16.8	52.40
Outer	60	Lignin	60.2	52.40
Outer	60	Lipid	5.0	52.40
Outer	60	Carbonyl	0.0	52.40
Outer	100	Carbohydrate	18.1	53.60
Outer	100	Protein	16.8	53.60
Outer	100	Lignin	60.2	53.60
Outer	100	Lipid	5.0	53.60
Outer	100	Carbonyl	0.0	53.60
Outer	180	Carbohydrate	22.4	39.96
Outer	180	Protein	9.4	39.96
Outer	180	Lignin	68.2	39.96
Outer	180	Lipid	0.0	39.96
Outer	180	Carbonyl	0.0	39.96
Outer	200	Carbohydrate	21.0	45.03
Outer	200	Protein	7.5	45.03
Outer	200	Lignin	69.4	45.03

Outer	200	Lipid	0.0	45.03
Outer	200	Carbonyl	2.2	45.03

410

Fig A1

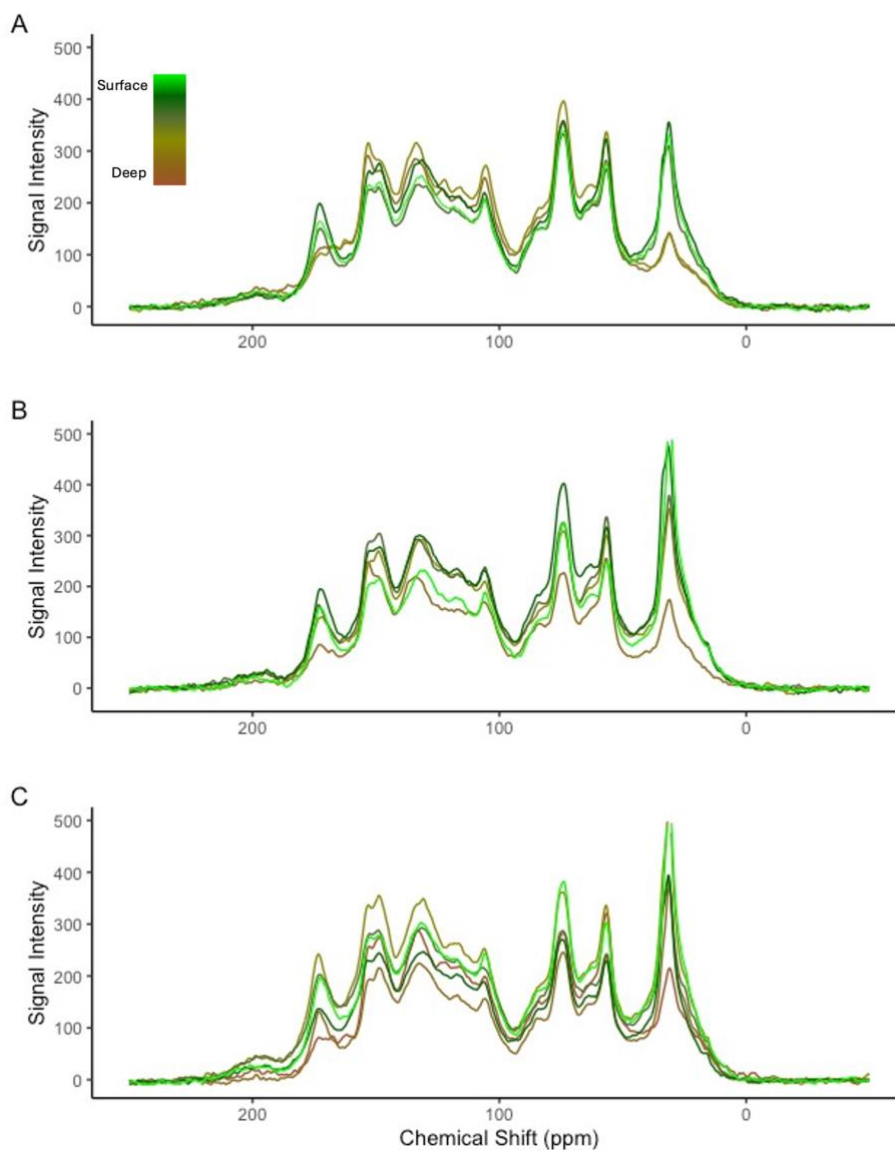


Fig A1: Stacked overlay of depth profiles of ¹³C NMR spectra of the A) Outer, B) Intermediate, and C) Inner site. Colors increase in darkness representing an increase in depth with light greens representing the surface peat soil, and dark browns representing deeper and the basal (deepest) peat soil. Peak areas were integrated corresponding to; alkyl C (0–45 ppm), N-alkyl/methoxyl C (45–60 ppm), O-alkyl C (60–95 ppm), di-O-alkyl (95–110), aromatic C (110–145 ppm), phenolic C (145–165 ppm), and carboxyl C (165–215 ppm). Overall, there are very similar peak heights and areas between depths and sites, with some differences in deep peat chemistry.

Fig A2

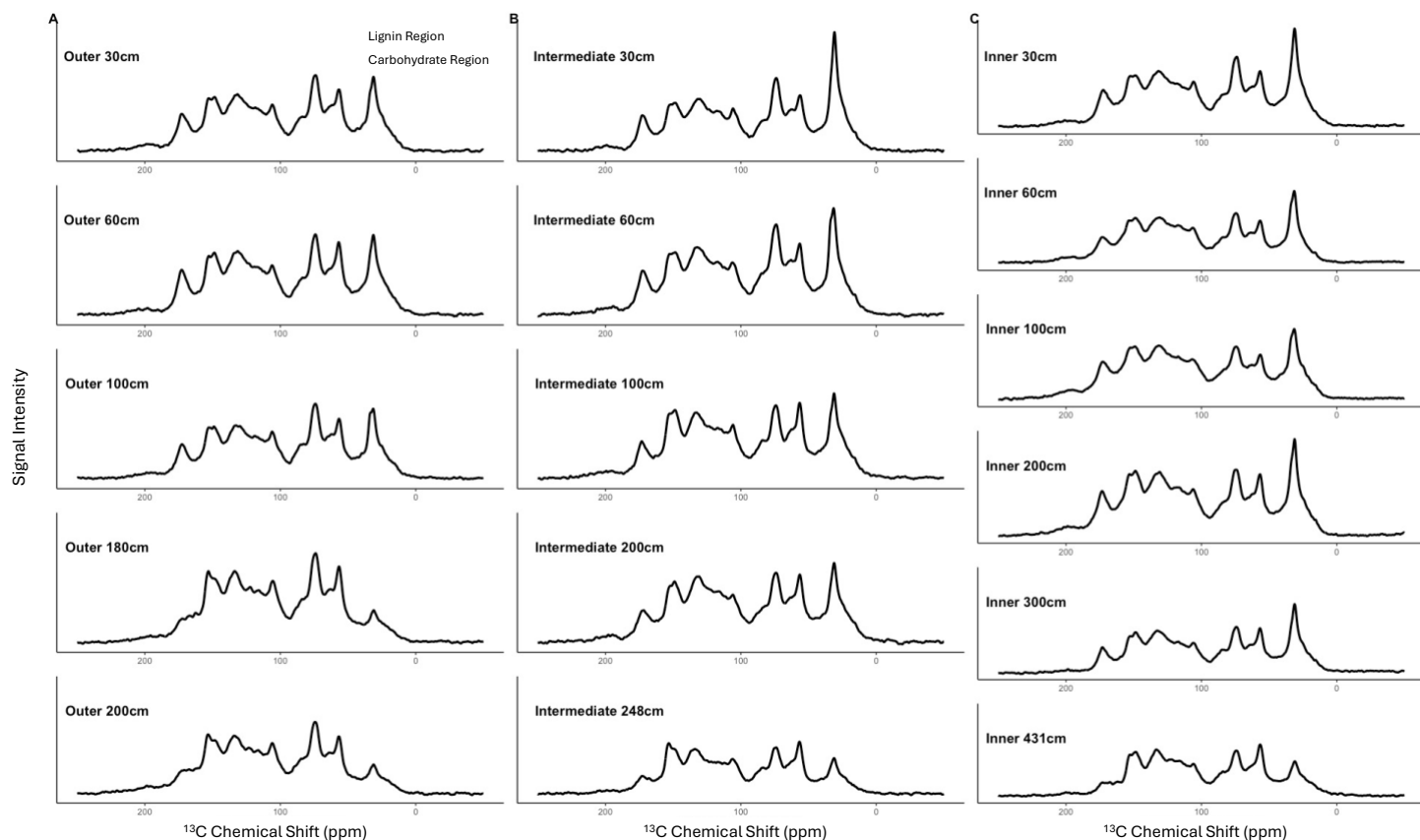


Fig A2: The ^{13}C NMR spectra of solid peat samples are shown across depth profiles for the A) Outer, B) Intermediate, and C) Inner peatland sites. Peak areas have been highlighted to emphasize changes in lignin (dark green range from 100-150ppm) and carbohydrate (light green, range from 60-105 ppm) across sites and depth. The y-axis has been scaled equally across all plots to visually compare changes in peak heights and area across depth, however the additional depths at the Inner site need to be considered when making this comparison. Overall, there are very similar peak heights and areas between depths and sites, with some differences in deep peat chemistry.

420 **Table A3: Results from t-tests** comparing bulk peat radiocarbon values versus respiration product gas radiocarbon values, and DOC radiocarbon values versus respiration product gas radiocarbon values. Solid peat samples had radiocarbon values significantly different from radiocarbon of gases, while soil DOC radiocarbon values were not different from those for gases.

	Sample Type	Mean	t-value	df	p-value
Pair 1	Bulk Peat	-96.56	-8.67	15.97	>0.001
	Gases (CH ₄ , CO ₂)	7.95			
Pair 2	DOC	2.03	0.54	23	0.60
	Gases (CH ₄ , CO ₂)	-3.88			

Fig A3

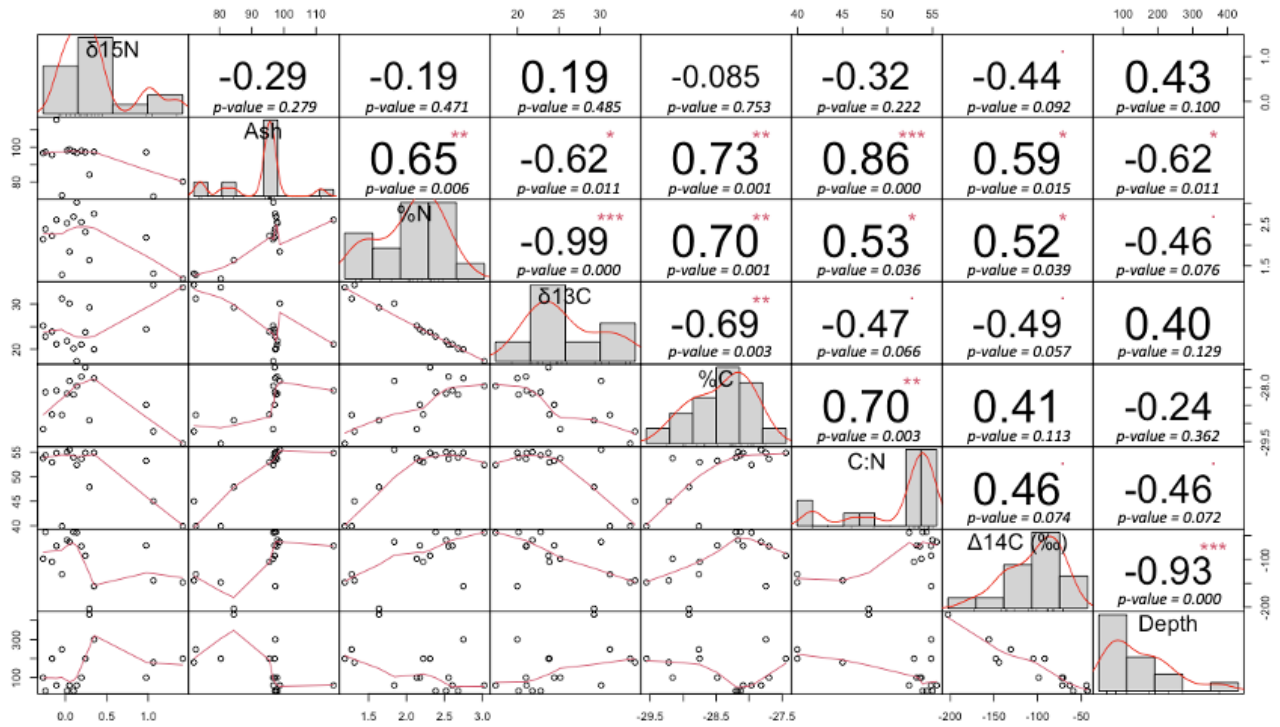


Fig A3: Correlation matrix for peat physical properties and depth. The numbers represent the value of the correlation coefficient (r) plus the result of the correlation test as stars. On the bottom of the matrix are the bivariate scatterplots with a fitted line. Significance levels are: >0 '***'; >0.001 '**'; >0.01 '*'; <0.1 ''

Fig A4

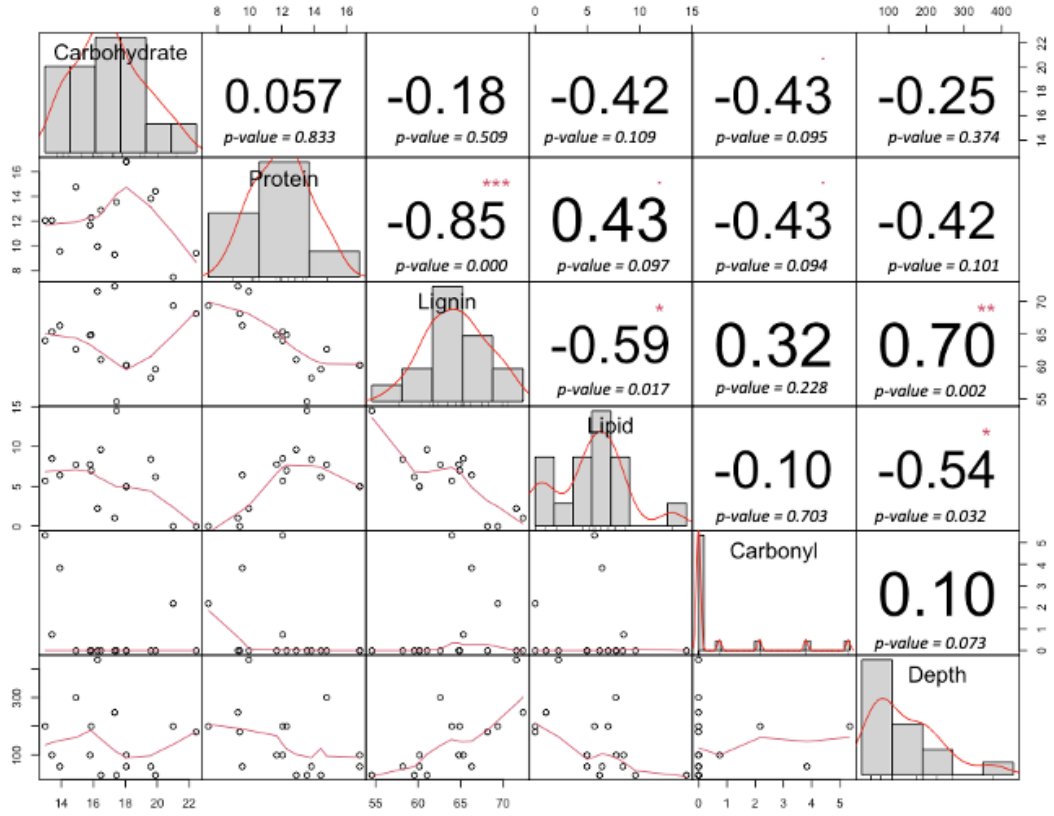


Fig A4: Correlation matrix for peat molecular components and depth. The numbers represent the value of the correlation (r^2) plus the result of the correlation test as stars. On the bottom of the matrix are bivariate scatterplots with a fitted line. Significance levels are: >0 ‘***’ ; >0.001 ‘**’ >0.01 ‘*’ <0.1 ‘

Table A4: PCA eigenvalues and loadings for PC1 and PC2. The top positive and negative loadings on each axis have been identified in bold.

	PC1	PC2
Eigenvalues	3.31	1.94
<i>Variable</i>		
$\delta^{15}\text{N}$	-0.19	0.04
Ash	-0.39	-0.08
%N	0.27	-0.11
$\delta^{13}\text{C}$	0.23	0.17
%C	0.26	0.09
C:N	-0.27	0.14
$\Delta^{14}\text{C}$ (‰)	0.23	0.04
Depth	-0.19	0.01
LOI	0.27	-0.01
Alkyl	0.28	-0.04
N-Alkyl/Methoxyl	-0.13	-0.40
O-Alkyl	-0.16	-0.33
Di_O_Alkyl	-0.27	-0.03
Aromatic	-0.25	0.03
Phenolic	-0.23	0.30
Amide/Carboxyl	0.09	0.41
Carbohydrate	-0.12	-0.34
Protein	0.24	-0.20
Lignin	-0.26	0.16
Lipid	0.26	-0.02
Carbonyl	-0.01	0.46

Fig A5

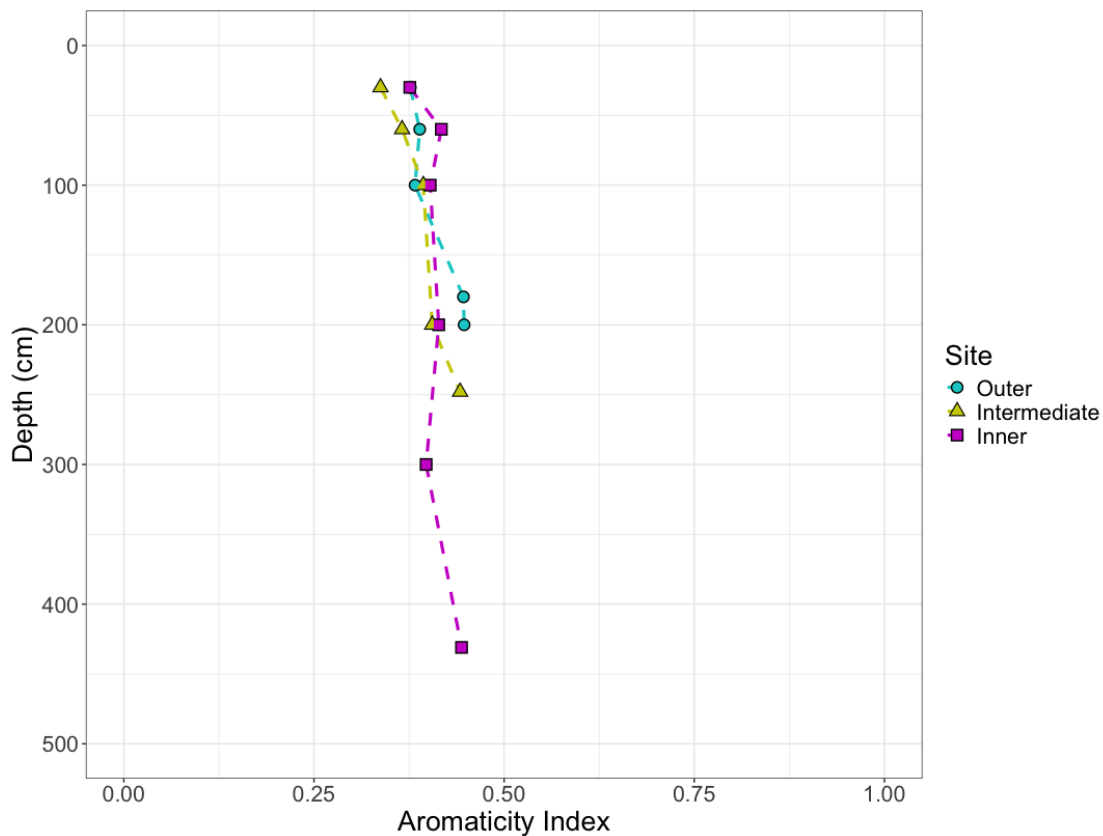


Fig A5: Aromaticity Index. The aromaticity index has been used to describe decomposition state of soils. This index is expressed as the ratio of Aromatic-C to Alkyl + O-Alkyl + Aromatic C, and is calculated using the results from integration of the ^{13}C NMR spectral regions. As the aromaticity index approaches 1, the soil is considered more decomposed. The lack of change in aromaticity with depth, and the consistency across all three sites, suggests that little decomposition has occurred over space and time. Sites are indicated by color and shape with blue circles indicating the outer site, yellow triangles the intermediate site, and pink squares the inner site.

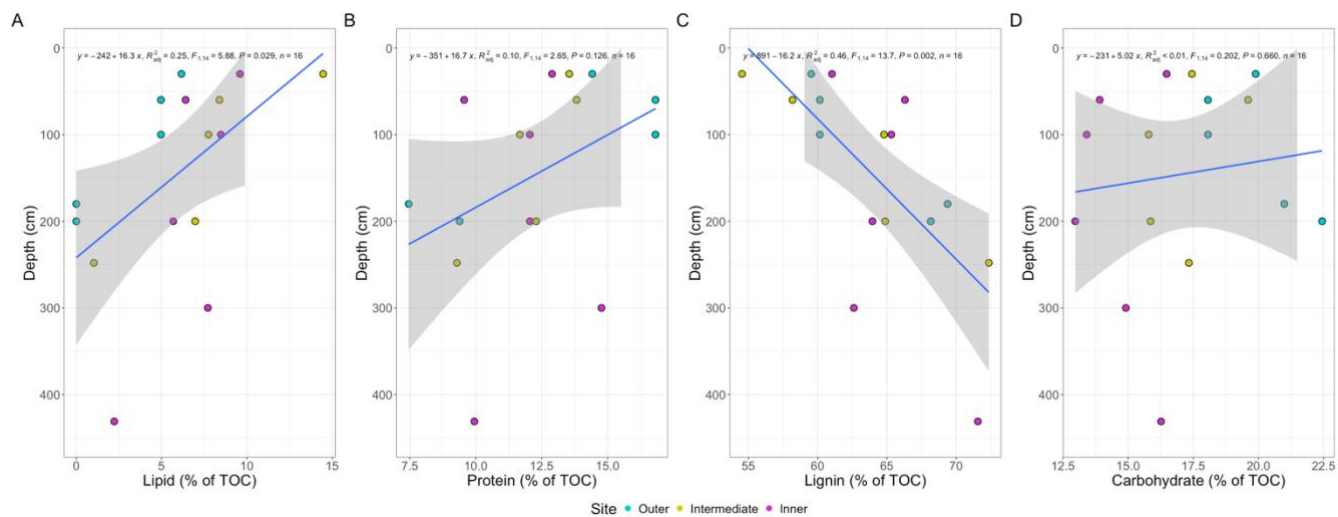


Fig A6: Linear regression of the four most abundant soil biomolecules from the mixing model versus depth. Sites have been pooled for this analysis and are indicated by color with blue indicating the outer site, yellow the intermediate site, and pink the inner site. Regressions show significant declines with depth for lipids, and significant increases with depth for lignin across sites.

Author Contribution

Alexandra Hedgpeth: Conceptualization; funding acquisition; data collection; formal analysis; investigation; methodology; visualization; writing – original draft. **Alison Hoyt:** Methodology; resources; formal analysis; visualization; supervision; writing – review and editing. **Daniela Cusack:** Conceptualization; funding acquisition; methodology; supervision; visualization; writing – review and editing. **Kyle Cavanaugh:** Supervision; writing – review and editing. **Karis McFarlane:** Funding acquisition; resources; methodology; supervision; writing – review and editing. Karis J. McFarlane and Daniela F. Cusack should be considered joint senior authors.

445 Data Availability

Following publication, the data that supports this manuscript will be publicly available at the US Department of Energy’s Environmental Systems Science Data Infrastructure for a Virtual Ecosystem (ESS-DIVE: <https://ess-dive.lbl.gov/>) and will be submitted to the International Soil Radiocarbon Database (<https://soilradiocarbon.org/>).

450 Competing interests

The contact author has declared that none of the authors has any competing interests.

Acknowledgements

A. Hedgpeth thanks the Smithsonian Tropical Research Institute for a short-term research fellowship, Eric Brown for field support, and the staff at the Smithsonian Tropical Research Institute and the Bocas del Toro field station for logistical support. This project was supported in part by a University of California-National Lab In-Residence Graduate Fellowship (#L21GF3629) to A. Hedgpeth, which was hosted by Lawrence Livermore National Laboratory. The ^{13}C -NMR analysis for this work was supported under a U.S. Department of Energy User Award (#60514) to D.F. Cusack and A. Hedgpeth, which was conducted at the Environmental Molecular Sciences Laboratory. Access to field and lab sites in Panama was supported by DOE Office of Science Early Career Award DE-SC0015898 and NSF Geography & Spatial Studies Grant #BCS-1437591 to D.F. Cusack. We would like to thank Sarah Burton and Andrew Lipton from the Environmental Molecular Sciences Laboratory for their assistance with the ^{13}C -NMR analysis. A portion of this work was performed under the auspices of the U.S. Department of Energy by Lawrence Livermore National Laboratory (LLNL-JRNL-868401) under Contract DE-AC52-07NA27344 and funded by the U.S. Department of Energy Office of Science Early Career Program Award (#SCW1572) to K. McFarlane. A.Hoyt was supported in part by the National Science Foundation (award 2406964). A. Hedgpeth would like to express appreciation for her dissertation committee members Glen MacDonald and Thomas Gillespie for their guidance, feedback, and support throughout the research process. We would like to thank Antonia L. Herwig, Lee Dietterich, and Makenna Brown for their assistance in the field.

References

- 470 Aliev, A. E.: Solid state NMR spectroscopy, in: Nuclear Magnetic Resonance, edited by: Hodgkinson, P., The Royal Society of Chemistry, 139–187, <https://doi.org/10.1039/9781788010665-00139>, 2020.
- Anderson, J. A. R. and Muller, J.: Palynological study of a holocene peat and a miocene coal deposit from NW Borneo, *Review of Palaeobotany and Palynology*, 19, 291–351, [https://doi.org/10.1016/0034-6667\(75\)90049-4](https://doi.org/10.1016/0034-6667(75)90049-4), 1975.
- 475 Aravena, R., Warner, B. G., Charman, D. J., Belyea, L. R., Mathur, S. P., and Diné, H.: Carbon Isotopic Composition of Deep Carbon Gases in an Ombrogenous Peatland, Northwestern Ontario, Canada, *Radiocarbon*, 35, 271–276, <https://doi.org/10.1017/S0033822200064948>, 1993.
- Bader, C., Müller, M., Schulin, R., and Leifeld, J.: Peat decomposability in managed organic soils in relation to land use, organic matter composition and temperature, *Biogeosciences*, 15, 703–719, <https://doi.org/10.5194/bg-15-703-2018>, 2018.
- 480 Baldock, J. A., Masiello, C. A., Gélinas, Y., and Hedges, J. I.: Cycling and composition of organic matter in terrestrial and marine ecosystems, *Marine Chemistry*, 92, 39–64, <https://doi.org/10.1016/j.marchem.2004.06.016>, 2004.
- Barreto, C. and Lindo, Z.: Decomposition in Peatlands: Who Are the Players and What Affects Them?, *Front. Young Minds*, 8, 107, <https://doi.org/10.3389/frym.2020.00107>, 2020.
- 485 Beilman, D. W., Massa, C., Nichols, J. E., Elison Timm, O., Kallstrom, R., and Dunbar-Co, S.: Dynamic Holocene Vegetation and North Pacific Hydroclimate Recorded in a Mountain Peatland, Moloka'i, Hawai'i, *Front. Earth Sci.*, 7, 188, <https://doi.org/10.3389/feart.2019.00188>, 2019.
- Blaauw, M. and Christen, J. A.: Flexible paleoclimate age-depth models using an autoregressive gamma process, *Bayesian Anal.*, 6, <https://doi.org/10.1214/11-BA618>, 2011.
- 490 Broek, T. A. B., Ognibene, T. J., McFarlane, K. J., Moreland, K. C., Brown, T. A., and Bench, G.: Conversion of the LLNL/CAMS 1 MV biomedical AMS system to a semi-automated natural abundance ¹⁴C spectrometer: system optimization and performance evaluation, *Nuclear Instruments and Methods in Physics Research Section B: Beam Interactions with Materials and Atoms*, 499, 124–132, <https://doi.org/10.1016/j.nimb.2021.01.022>, 2021.
- Chanton, J. P., Bauer, J. E., Glaser, P. A., Siegel, D. I., Kelley, C. A., Tyler, S. C., Romanowicz, E. H., and Lazrus, A.: Radiocarbon evidence for the substrates supporting methane formation within northern Minnesota peatlands, *Geochimica et Cosmochimica Acta*, 59, 3663–3668, [https://doi.org/10.1016/0016-7037\(95\)00240-Z](https://doi.org/10.1016/0016-7037(95)00240-Z), 1995.
- 495 Chanton, J. P., Glaser, P. H., Chasar, L. S., Burdige, D. J., Hines, M. E., Siegel, D. I., Tremblay, L. B., and Cooper, W. T.: Radiocarbon evidence for the importance of surface vegetation on fermentation and methanogenesis in contrasting types of boreal peatlands, *Global Biogeochemical Cycles*, 22, 2008GB003274, <https://doi.org/10.1029/2008GB003274>, 2008.
- Clymo, R. S., Turunen, J., and Tolonen, K.: Carbon Accumulation in Peatland, *Oikos*, 81, 368, <https://doi.org/10.2307/3547057>, 1998.
- 500 Cobb, A. R., Hoyt, A. M., Gandois, L., Eri, J., Dommain, R., Abu Salim, K., Kai, F. M., Haji Su'ut, N. S., and Harvey, C. F.: How temporal patterns in rainfall determine the geomorphology and carbon fluxes of tropical peatlands, *Proc. Natl. Acad. Sci. U.S.A.*, 114, <https://doi.org/10.1073/pnas.1701090114>, 2017.
- Cobb, A. R., Dommain, R., Yeap, K., Hannan, C., Dadap, N. C., Bookhagen, B., Glaser, P. H., and Harvey, C. F.: A unified explanation for the morphology of raised peatlands, *Nature*, 625, 79–84, <https://doi.org/10.1038/s41586-023-06807-w>, 2024.

- 505 Cohen, A. D., Raymond, R., Ramirez, A., Morales, Z., and Ponce, F.: The Changuinola peat deposit of northwestern Panama: a tropical, back-barrier, peat(coal)-forming environment, *International Journal of Coal Geology*, 12, 157–192, [https://doi.org/10.1016/0166-5162\(89\)90050-5](https://doi.org/10.1016/0166-5162(89)90050-5), 1989.
- Conrad, R.: Importance of hydrogenotrophic, acetoclastic and methylotrophic methanogenesis for methane production in terrestrial, aquatic and other anoxic environments: A mini review, *Pedosphere*, 30, 25–39, [https://doi.org/10.1016/S1002-0160\(18\)60052-9](https://doi.org/10.1016/S1002-0160(18)60052-9), 2020.
- 510 Corbett, J. E., Tfaily, M. M., Burdige, D. J., Cooper, W. T., Glaser, P. H., and Chanton, J. P.: Partitioning pathways of CO₂ production in peatlands with stable carbon isotopes, *Biogeochemistry*, 114, 327–340, <https://doi.org/10.1007/s10533-012-9813-1>, 2013.
- Cusack, D. F., Markesteijn, L., Condit, R., Lewis, O. T., and Turner, B. L.: Soil carbon stocks across tropical forests of Panama regulated by base cation effects on fine roots, *Biogeochemistry*, 137, 253–266, <https://doi.org/10.1007/s10533-017-0416-8>, 2018.
- 515 Dargie, G. C., Lewis, S. L., Lawson, I. T., Mitchard, E. T. A., Page, S. E., Bocko, Y. E., and Ifo, S. A.: Age, extent and carbon storage of the central Congo Basin peatland complex, *Nature*, 542, 86–90, <https://doi.org/10.1038/nature21048>, 2017.
- Dhandapani, S., Girkin, N. T., and Evers, S.: Spatial variability of surface peat properties and carbon emissions in a tropical peatland oil palm monoculture during a dry season, *Soil Use and Management*, 38, 381–395, <https://doi.org/10.1111/sum.12741>, 2022.
- 520 Dhandapani, S., Evers, S., Boyd, D., Evans, C. D., Page, S., Parish, F., and Sjögersten, S.: Assessment of differences in peat physico-chemical properties, surface subsidence and GHG emissions between the major land-uses of Selangor peatlands, *CATENA*, 230, 107255, <https://doi.org/10.1016/j.catena.2023.107255>, 2023.
- Dommain, R., Couwenberg, J., and Joosten, H.: Development and carbon sequestration of tropical peat domes in south-east Asia: links to post-glacial sea-level changes and Holocene climate variability, *Quaternary Science Reviews*, 30, 999–1010, <https://doi.org/10.1016/j.quascirev.2011.01.018>, 2011.
- 525 Dommain, R., Cobb, A. R., Joosten, H., Glaser, P. H., Chua, A. F. L., Gandois, L., Kai, F., Noren, A., Salim, K. A., Su'ut, N. S. H., and Harvey, C. F.: Forest dynamics and tip-up pools drive pulses of high carbon accumulation rates in a tropical peat dome in Borneo (Southeast Asia), *JGR Biogeosciences*, 120, 617–640, <https://doi.org/10.1002/2014JG002796>, 2015.
- 530 Farmer, J., Matthews, R., Smith, J. U., Smith, P., and Singh, B. K.: Assessing existing peatland models for their applicability for modelling greenhouse gas emissions from tropical peat soils, *Current Opinion in Environmental Sustainability*, 3, 339–349, <https://doi.org/10.1016/j.cosust.2011.08.010>, 2011.
- Fritts, R.: Tropical Wetlands Emit More Methane Than Previously Thought, *Eos*, 103, <https://doi.org/10.1029/2022EO220443>, 2022.
- 535 Gandois, L., Teisserenc, R., Cobb, A. R., Chieng, H. I., Lim, L. B. L., Kamariah, A. S., Hoyt, A., and Harvey, C. F.: Origin, composition, and transformation of dissolved organic matter in tropical peatlands, *Geochimica et Cosmochimica Acta*, 137, 35–47, <https://doi.org/10.1016/j.gca.2014.03.012>, 2014.
- Girkin, N. T., Turner, B. L., Ostle, N., Craigon, J., and Sjögersten, S.: Root exudate analogues accelerate CO₂ and CH₄ production in tropical peat, *Soil Biology and Biochemistry*, 117, 48–55, <https://doi.org/10.1016/j.soilbio.2017.11.008>, 2018.
- 540

- Girkin, N. T., Vane, C. H., Cooper, H. V., Moss-Hayes, V., Craighan, J., Turner, B. L., Ostle, N., and Sjögersten, S.: Spatial variability of organic matter properties determines methane fluxes in a tropical forested peatland, *Biogeochemistry*, 142, 231–245, <https://doi.org/10.1007/s10533-018-0531-1>, 2019.
- 545 Girkin, N. T., Dhandapani, S., Evers, S., Ostle, N., Turner, B. L., and Sjögersten, S.: Interactions between labile carbon, temperature and land use regulate carbon dioxide and methane production in tropical peat, *Biogeochemistry*, 147, 87–97, <https://doi.org/10.1007/s10533-019-00632-y>, 2020.
- Girkin, N. T., Cooper, H. V., Ledger, M. J., O'Reilly, P., Thornton, S. A., Åkesson, C. M., Cole, L. E. S., Hapsari, K. A., Hawthorne, D., and Roucoux, K. H.: Tropical peatlands in the Anthropocene: The present and the future, *Anthropocene*, 40, 100354, <https://doi.org/10.1016/j.ancene.2022.100354>, 2022.
- 550 Goldstein, A., Turner, W. R., Spawn, S. A., Anderson-Teixeira, K. J., Cook-Patton, S., Fargione, J., Gibbs, H. K., Griscom, B., Hewson, J. H., Howard, J. F., Ledezma, J. C., Page, S., Koh, L. P., Rockström, J., Sanderman, J., and Hole, D. G.: Protecting irrecoverable carbon in Earth's ecosystems, *Nat. Clim. Chang.*, 10, 287–295, <https://doi.org/10.1038/s41558-020-0738-8>, 2020.
- 555 Gruca-Rokosz, R. and Koszelnik, P.: Production pathways for CH₄ and CO₂ in sediments of two freshwater ecosystems in south-eastern Poland, *PLoS ONE*, 13, e0199755, <https://doi.org/10.1371/journal.pone.0199755>, 2018.
- Hirano, T., Jauhiainen, J., Inoue, T., and Takahashi, H.: Controls on the Carbon Balance of Tropical Peatlands, *Ecosystems*, 12, 873–887, <https://doi.org/10.1007/s10021-008-9209-1>, 2009.
- 560 Hodgkins, S. B., Richardson, C. J., Dommain, R., Wang, H., Glaser, P. H., Verbeke, B., Winkler, B. R., Cobb, A. R., Rich, V. I., Missilmani, M., Flanagan, N., Ho, M., Hoyt, A. M., Harvey, C. F., Vining, S. R., Hough, M. A., Moore, T. R., Richard, P. J. H., De La Cruz, F. B., Toufaily, J., Hamdan, R., Cooper, W. T., and Chanton, J. P.: Tropical peatland carbon storage linked to global latitudinal trends in peat recalcitrance, *Nat Commun*, 9, 3640, <https://doi.org/10.1038/s41467-018-06050-2>, 2018.
- Holmes, M. E., Chanton, J. P., Tfaily, M. M., and Ogram, A.: CO₂ and CH₄ isotope compositions and production pathways in a tropical peatland, *Global Biogeochemical Cycles*, 29, 1–18, <https://doi.org/10.1002/2014GB004951>, 2015.
- 565 Hornibrook, E. R. C., Longstaffe, F. J., and Fyfe, W. S.: Evolution of stable carbon isotope compositions for methane and carbon dioxide in freshwater wetlands and other anaerobic environments, *Geochimica et Cosmochimica Acta*, 64, 1013–1027, [https://doi.org/10.1016/S0016-7037\(99\)00321-X](https://doi.org/10.1016/S0016-7037(99)00321-X), 2000.
- Hoyos-Santillan, J.: 2014 Hoyos Controls of Carbon Turnover in Tropical Peatlands, <https://doi.org/10.13140/2.1.3387.2329>, 2014.
- 570 Hoyos-Santillan, J., Lomax, B. H., Large, D., Turner, B. L., Boom, A., Lopez, O. R., and Sjögersten, S.: Getting to the root of the problem: litter decomposition and peat formation in lowland Neotropical peatlands, *Biogeochemistry*, 126, 115–129, <https://doi.org/10.1007/s10533-015-0147-7>, 2015.
- Hoyos-Santillan, J., Lomax, B. H., Large, D., Turner, B. L., Boom, A., Lopez, O. R., and Sjögersten, S.: Quality not quantity: Organic matter composition controls of CO₂ and CH₄ fluxes in neotropical peat profiles, *Soil Biology and Biochemistry*, 103, 86–96, <https://doi.org/10.1016/j.soilbio.2016.08.017>, 2016.
- 575 Hoyos-Santillan, J., Lomax, B. H., Large, D., Turner, B. L., Lopez, O. R., Boom, A., Sepulveda-Jauregui, A., and Sjögersten, S.: Evaluation of vegetation communities, water table, and peat composition as drivers of greenhouse gas emissions in lowland tropical peatlands, *Science of The Total Environment*, 688, 1193–1204, <https://doi.org/10.1016/j.scitotenv.2019.06.366>, 2019.

- Hoyt, A.: Methane production and transport in a tropical peatland, AGU Fall Meeting Abstracts, 2014.
- 580 Hoyt, A., Cadillo-Quiroz, H., Xu, X., Torn, M., Bazán Pacaya, A., Jacobs, M., Shapiama Peña, R., Ramirez Navarro, D., Urquiza-Muñoz, D., and Trumbore, S.: Isotopic Insights into Methane Production and Emission in Diverse Amazonian Peatlands, oral, <https://doi.org/10.5194/egusphere-egu2020-12960>, 2020.
- Hoyt, A. M., Gandois, L., Eri, J., Kai, F. M., Harvey, C. F., and Cobb, A. R.: CO₂ emissions from an undrained tropical peatland: Interacting influences of temperature, shading and water table depth, *Global Change Biology*, 25, 2885–2899, <https://doi.org/10.1111/gcb.14702>, 2019.
- 585 Ingram, H. A. P.: Ecohydrology of Scottish peatlands, *Transactions of the Royal Society of Edinburgh: Earth Sciences*, 78, 287–296, <https://doi.org/10.1017/S0263593300011226>, 1987.
- Jastrow, J. D., Amonette, J. E., and Bailey, V. L.: Mechanisms controlling soil carbon turnover and their potential application for enhancing carbon sequestration, *Climatic Change*, 80, 5–23, <https://doi.org/10.1007/s10584-006-9178-3>, 2007.
- 590 Jauhiainen, J., Takahashi, H., Heikkinen, J. E. P., Martikainen, P. J., and Vasander, H.: Carbon fluxes from a tropical peat swamp forest floor, *Global Change Biology*, 11, 1788–1797, <https://doi.org/10.1111/j.1365-2486.2005.001031.x>, 2005.
- Jauhiainen, J., Kerojoki, O., Silvennoinen, H., Limin, S., and Vasander, H.: Heterotrophic respiration in drained tropical peat is greatly affected by temperature—a passive ecosystem cooling experiment, *Environ. Res. Lett.*, 9, 105013, <https://doi.org/10.1088/1748-9326/9/10/105013>, 2014.
- 595 Kettridge, N., Turetsky, M. R., Sherwood, J. H., Thompson, D. K., Miller, C. A., Benscoter, B. W., Flannigan, M. D., Wotton, B. M., and Waddington, J. M.: Moderate drop in water table increases peatland vulnerability to post-fire regime shift, *Sci Rep*, 5, 8063, <https://doi.org/10.1038/srep08063>, 2015.
- Kotsyurbenko, O. R., Chin, K.-J., Glagolev, M. V., Stubner, S., Simankova, M. V., Nozhevnikova, A. N., and Conrad, R.: Acetoclastic and hydrogenotrophic methane production and methanogenic populations in an acidic West-Siberian peat bog, *Environ Microbiol*, 6, 1159–1173, <https://doi.org/10.1111/j.1462-2920.2004.00634.x>, 2004.
- 600 Lähteenoja, O., Reátegui, Y. R., Räsänen, M., Torres, D. D. C., Oinonen, M., and Page, S.: The large Amazonian peatland carbon sink in the subsiding Pastaza-Marañón foreland basin, Peru, *Global Change Biology*, 18, 164–178, <https://doi.org/10.1111/j.1365-2486.2011.02504.x>, 2012.
- Lampela, M., Jauhiainen, J., and Vasander, H.: Surface peat structure and chemistry in a tropical peat swamp forest, *Plant Soil*, 382, 329–347, <https://doi.org/10.1007/s11104-014-2187-5>, 2014.
- 605 Liebner, S., Ganzert, L., Kiss, A., Yang, S., Wagner, D., and Svenning, M. M.: Shifts in methanogenic community composition and methane fluxes along the degradation of discontinuous permafrost, *Front. Microbiol.*, 6, <https://doi.org/10.3389/fmicb.2015.00356>, 2015.
- 610 Loisel, J., Gallego-Sala, A. V., Amesbury, M. J., Magnan, G., Anshari, G., Beilman, D. W., Benavides, J. C., Blewett, J., Camill, P., Charman, D. J., Chawchai, S., Hedgpeth, A., Kleinen, T., Korhola, A., Large, D., Mansilla, C. A., Müller, J., Van Bellen, S., West, J. B., Yu, Z., Bubier, J. L., Garneau, M., Moore, T., Sannel, A. B. K., Page, S., Väliranta, M., Bechtold, M., Brovkin, V., Cole, L. E. S., Chanton, J. P., Christensen, T. R., Davies, M. A., De Vleeschouwer, F., Finkelstein, S. A., Frolking, S., Galka, M., Gandois, L., Girkin, N., Harris, L. I., Heinemeyer, A., Hoyt, A. M., Jones, M. C., Joos, F., Juutinen, S., Kaiser, K., Lacourse, T., Lamentowicz, M., Larmola, T., Leifeld, J., Lohila, A., Milner, A. M., Minkinen, K., Moss, P., Naafs, B. D. A., Nichols, J., O'Donnell, J., Payne, R., Philben, M., Piilo, S., Quillet, A., Ratnayake, A. S., Roland, T. P., Sjögersten, S., 615 Sonnentag, O., Swindles, G. T., Swinnen, W., Talbot, J., Treat, C., Valach, A. C., and Wu, J.: Expert assessment of future

- vulnerability of the global peatland carbon sink, *Nat. Clim. Chang.*, 11, 70–77, <https://doi.org/10.1038/s41558-020-00944-0>, 2021.
- 620 McNicol, G., Knox, S. H., Guilderson, T. P., Baldocchi, D. D., and Silver, W. L.: Where old meets new: An ecosystem study of methanogenesis in a reflooded agricultural peatland, *Global Change Biology*, 26, 772–785, <https://doi.org/10.1111/gcb.14916>, 2020.
- Mobilian, C. and Craft, C. B.: Wetland Soils: Physical and Chemical Properties and Biogeochemical Processes, in: *Encyclopedia of Inland Waters*, Elsevier, 157–168, <https://doi.org/10.1016/B978-0-12-819166-8.00049-9>, 2022.
- 625 Moore, S., Evans, C. D., Page, S. E., Garnett, M. H., Jones, T. G., Freeman, C., Hooijer, A., Wiltshire, A. J., Limin, S. H., and Gauci, V.: Deep instability of deforested tropical peatlands revealed by fluvial organic carbon fluxes, *Nature*, 493, 660–663, <https://doi.org/10.1038/nature11818>, 2013.
- Noon, M. L., Goldstein, A., Ledezma, J. C., Roehrdanz, P. R., Cook-Patton, S. C., Spawn-Lee, S. A., Wright, T. M., Gonzalez-Roglich, M., Hole, D. G., Rockström, J., and Turner, W. R.: Mapping the irrecoverable carbon in Earth’s ecosystems, *Nat Sustain*, 5, 37–46, <https://doi.org/10.1038/s41893-021-00803-6>, 2021.
- 630 Norris, M. W., Turnbull, J. C., Howarth, J. D., and Vandergoes, M. J.: Pretreatment of Terrestrial Macrofossils, *Radiocarbon*, 62, 349–360, <https://doi.org/10.1017/RDC.2020.8>, 2020.
- Nottingham, A. T., Bååth, E., Reischke, S., Salinas, N., and Meir, P.: Adaptation of soil microbial growth to temperature: Using a tropical elevation gradient to predict future changes, *Global Change Biology*, 25, 827–838, <https://doi.org/10.1111/gcb.14502>, 2019.
- 635 Omar, M. S., Ifandi, E., Sukri, R. S., Kalaitzidis, S., Christanis, K., Lai, D. T. C., Bashir, S., and Tsikouras, B.: Peatlands in Southeast Asia: A comprehensive geological review, *Earth-Science Reviews*, 232, 104149, <https://doi.org/10.1016/j.earscirev.2022.104149>, 2022.
- Osaki, M., Kato, T., Kohyama, T., Takahashi, H., Haraguchi, A., Yabe, K., Tsuji, N., Shiodera, S., Rahajoe, J. S., Atikah, T. D., Oide, A., Matsui, K., Wetadewi, R. I., and Silsigia, S.: Basic Information About Tropical Peatland Ecosystems, in: *Tropical Peatland Eco-management*, edited by: Osaki, M., Tsuji, N., Foead, N., and Rieley, J., Springer Singapore, Singapore, 3–62, https://doi.org/10.1007/978-981-33-4654-3_1, 2021.
- 640 Page, S. E., Rieley, J. O., and Banks, C. J.: Global and regional importance of the tropical peatland carbon pool, *Global Change Biology*, 17, 798–818, <https://doi.org/10.1111/j.1365-2486.2010.02279.x>, 2011.
- Phillips, S. and Bustin, R. M.: Sedimentology of the Changuinola peat deposit: Organic and clastic sedimentary response to punctuated coastal subsidence, *Geological Society of America Bulletin*, 108, 794–814, [https://doi.org/10.1130/0016-7606\(1996\)108<0794:SOTCPD>2.3.CO;2](https://doi.org/10.1130/0016-7606(1996)108<0794:SOTCPD>2.3.CO;2), 1996.
- 645 Phillips, S., Rouse, G. E., and Bustin, R. M.: Vegetation zones and diagnostic pollen profiles of a coastal peat swamp, Bocas del Toro, Panamá, *Palaeogeography, Palaeoclimatology, Palaeoecology*, 128, 301–338, [https://doi.org/10.1016/S0031-0182\(97\)81129-7](https://doi.org/10.1016/S0031-0182(97)81129-7), 1997.
- 650 Ribeiro, K., Pacheco, F. S., Ferreira, J. W., De Sousa-Neto, E. R., Hastie, A., Krieger Filho, G. C., Alvalá, P. C., Forti, M. C., and Ometto, J. P.: Tropical peatlands and their contribution to the global carbon cycle and climate change, *Global Change Biology*, 27, 489–505, <https://doi.org/10.1111/gcb.15408>, 2021.

- Sjögersten, S., Cheesman, A. W., Lopez, O., and Turner, B. L.: Biogeochemical processes along a nutrient gradient in a tropical ombrotrophic peatland, *Biogeochemistry*, 104, 147–163, <https://doi.org/10.1007/s10533-010-9493-7>, 2011.
- 655 Stuver, M. and Polach, H. A.: Discussion Reporting of ^{14}C Data, *Radiocarbon*, 19, 355–363, <https://doi.org/10.1017/S0033822200003672>, 1977.
- Sugimoto, A. and Wada, E.: Carbon isotopic composition of bacterial methane in a soil incubation experiment: Contributions of acetate and, *Geochimica et Cosmochimica Acta*, 57, 4015–4027, [https://doi.org/10.1016/0016-7037\(93\)90350-6](https://doi.org/10.1016/0016-7037(93)90350-6), 1993.
- 660 Sun, C. L., Brauer, S. L., Cadillo-Quiroz, H., Zinder, S. H., and Yavitt, J. B.: Seasonal Changes in Methanogenesis and Methanogenic Community in Three Peatlands, New York State, *Front. Microbio.*, 3, <https://doi.org/10.3389/fmicb.2012.00081>, 2012.
- Thormann, M. N.: Diversity and function of fungi in peatlands: A carbon cycling perspective, *Can. J. Soil. Sci.*, 86, 281–293, <https://doi.org/10.4141/S05-082>, 2006.
- Troxler, T. G.: Patterns of phosphorus, nitrogen and $\delta^{15}\text{N}$ along a peat development gradient in a coastal mire, Panama, *J. Trop. Ecol.*, 23, 683–691, <https://doi.org/10.1017/S0266467407004464>, 2007.
- 665 Troxler, T. G., Ikenaga, M., Scinto, L., Boyer, J. N., Condit, R., Perez, R., Gann, G. D., and Childers, D. L.: Patterns of Soil Bacteria and Canopy Community Structure Related to Tropical Peatland Development, *Wetlands*, 32, 769–782, <https://doi.org/10.1007/s13157-012-0310-z>, 2012.
- United Nations Environment Programme, Global Environment Facility, Asia Pacific Network for Global Change Research, Global Environment Centre (Malaysia), and Wetlands International (Eds.): Assessment on peatlands, biodiversity, and climate change, Global Environment Centre & Wetlands International, Wageningen, Kuala Lumpur, 2 pp., 2008.
- 670 Upton, A., Vane, C. H., Girkin, N., Turner, B. L., and Sjögersten, S.: Does litter input determine carbon storage and peat organic chemistry in tropical peatlands?, *Geoderma*, 326, 76–87, <https://doi.org/10.1016/j.geoderma.2018.03.030>, 2018.
- Vogel, J. S., Southon, J. R., Nelson, D. E., and Brown, T. A.: Performance of catalytically condensed carbon for use in accelerator mass spectrometry, *Nuclear Instruments and Methods in Physics Research Section B: Beam Interactions with Materials and Atoms*, 5, 289–293, [https://doi.org/10.1016/0168-583X\(84\)90529-9](https://doi.org/10.1016/0168-583X(84)90529-9), 1984.
- 675 Wiesenberg, G. L. B., Dorodnikov, M., and Kuzyakov, Y.: Source determination of lipids in bulk soil and soil density fractions after four years of wheat cropping, *Geoderma*, 156, 267–277, <https://doi.org/10.1016/j.geoderma.2010.02.026>, 2010.
- Wilson, R. M., Hopple, A. M., Tfaily, M. M., Sebestyen, S. D., Schadt, C. W., Pfeifer-Meister, L., Medvedeff, C., McFarlane, K. J., Kostka, J. E., Kolton, M., Kolka, R. K., Kluber, L. A., Keller, J. K., Guilderson, T. P., Griffiths, N. A., Chanton, J. P., Bridgham, S. D., and Hanson, P. J.: Stability of peatland carbon to rising temperatures, *Nat Commun*, 7, 13723, <https://doi.org/10.1038/ncomms13723>, 2016.
- 680 Wilson, R. M., Griffiths, N. A., Visser, A., McFarlane, K. J., Sebestyen, S. D., Oleheiser, K. C., Bosman, S., Hopple, A. M., Tfaily, M. M., Kolka, R. K., Hanson, P. J., Kostka, J. E., Bridgham, S. D., Keller, J. K., and Chanton, J. P.: Radiocarbon Analyses Quantify Peat Carbon Losses With Increasing Temperature in a Whole Ecosystem Warming Experiment, *JGR Biogeosciences*, 126, e2021JG006511, <https://doi.org/10.1029/2021JG006511>, 2021.
- 685 Wright, E. L., Black, C. R., Cheesman, A. W., Drage, T., Large, D., Turner, B. L., and Sjögersten, S.: Contribution of subsurface peat to CO_2 and CH_4 fluxes in a neotropical peatland: CARBON FLUXES IN A NEOTROPICAL PEATLAND, *Global Change Biology*, 17, 2867–2881, <https://doi.org/10.1111/j.1365-2486.2011.02448.x>, 2011.

690 Wright, E. L., Black, C. R., Turner, B. L., and Sjögersten, S.: Environmental controls of temporal and spatial variability in
CO₂ and CH₄ fluxes in a neotropical peatland, *Global Change Biology*, 19, 3775–3789, <https://doi.org/10.1111/gcb.12330>,
2013.

Zhang, Y., Ma, A., Zhuang, G., and Zhuang, X.: The acetotrophic pathway dominates methane production in Zoige alpine
wetland coexisting with hydrogenotrophic pathway, *Sci Rep*, 9, 9141, <https://doi.org/10.1038/s41598-019-45590-5>, 2019.

695